

Challenges and opportunities for quantifying roots and rhizosphere interactions through imaging and image analysis

Downie, H.F., Adu, M.O., Schmidt, S., Otten, W., Dupuy, L.X., White, P.J. and Valentine, T.A.

This is the peer reviewed version of the following article:

Downie, H.F., et al. 2015. Challenges and opportunities for quantifying roots and rhizosphere interactions through imaging and image analysis. *Plant, Cell & Environment*. 38(7): pp.1213-1232.

which has been published in final form at <http://dx.doi.org/10.1111/pce.12448>

This article may be used for non-commercial purposes in accordance with Wiley Terms and Conditions for Self-Archiving

Some minor changes may have been introduced during type-setting and proofing.

1 **Challenges and opportunities for**
2 **quantifying roots and rhizosphere**
3 **interactions through imaging and image**
4 **analysis.**

5

6 Running Title: Quantifying the rhizosphere using image analysis

7

8 ^{*1,2,4}Downie, H.F., ^{*2,3}Adu, M.O., ^{*1}Schmidt, S., ¹Otten, W., ²Dupuy, L.X., ^{2,5}White, P.J. and
9 ²Valentine, T.A.

10 * These authors have contributed equally to this manuscript

11 ¹The SIMBIOS Centre, Abertay University, Dundee DD1 1HG.

12 ²Ecological Sciences, The James Hutton Institute, Invergowrie, Dundee DD2 5DA.

13 ³Plant and Crop Sciences Division, School of Biosciences, The University of
14 Nottingham, Sutton Bonington, Leicestershire LE12 5RD.

15 ⁴Current address: Williamson Research Centre for Molecular Environmental Science,
16 School of Earth, Atmospheric, and Environmental Sciences, The University of
17 Manchester, Manchester, United Kingdom.

18 ⁵King Saud University, Riyadh, Saudi Arabia.

19 Corresponding Author: Tracy A. Valentine,

20 Address: Ecological Sciences, The James Hutton Institute,
21 Invergowrie, Dundee DD2 5DA.

22 e-mail: Tracy.Valentine@hutton.ac.uk

23

24 **ABSTRACT**

25

26 The morphology of roots and root systems influences the efficiency by which plants acquire
27 nutrients and water, anchor themselves and provide stability to the surrounding soil. Plant
28 genotype and the biotic and abiotic environment significantly influence root morphology,
29 growth and ultimately crop yield. The challenge for researchers interested in phenotyping
30 root systems is, therefore, not just to measure roots and link their phenotype to the plant
31 genotype, but also to understand how the growth of roots is influenced by their environment.
32 This review discusses progress in quantifying root system parameters (e.g. in terms of size,
33 shape and dynamics) using imaging and image analysis technologies and also discusses their
34 potential for providing a better understanding of root:soil interactions. Significant progress
35 has been made in image acquisition techniques, however trade-offs exist between sample
36 throughput, sample size, image resolution and information gained. All of these factors impact
37 on downstream image analysis processes. While there have been significant advances in
38 computation power, limitations still exist in statistical processes involved in image analysis.
39 Utilizing and combining different imaging systems, integrating measurements and image
40 analysis where possible, and amalgamating data will allow researchers to gain a better
41 understanding of root:soil interactions.

42

43 *Key-words:* rhizosphere, root system architecture (RSA), image analysis, automation,
44 microscopy, computed tomography, abiotic interactions, biotic interactions, soil, root:soil
45 interactions.

46

47 INTRODUCTION

48 An increasing world population that is estimated to reach 9.6 billion by 2050 (United Nations,
49 2013) and changes in dietary choices, including increased meat consumption, has resulted in
50 unprecedented food, and therefore crop production demands (Tilman et al., 2011, White et al.,
51 2013b). In addition many of the crop producing regions of the world are experiencing
52 unfavourable environmental conditions such as drought or flooding and agricultural land is
53 under pressure due to competition for the production of biofuels (Valentine et al., 2012a).
54 Currently, crop production in many regions relies heavily on mineral fertilisers, however,
55 mineral resources for the production of these fertilisers are finite and the production process
56 relies heavily on fossil fuels (White et al., 2013a). The global nutrient use efficiency (NUE)
57 for nitrogen, phosphorus and potassium has been estimated at 50%, 40% and 75%
58 respectively, and there is therefore significant scope for improvement in fertilizer use
59 efficiency (Tan et al., 2005). In addition, crop production must be maintained for the long-
60 term, so crop improvement objectives must either maintain crop yields with reduced inputs or
61 increase yield under intensive agricultural practices while avoiding long-term ecological
62 damage (Gomiero et al., 2011). Since roots of crop plants are responsible for the uptake of
63 resources from the soil, an understanding of the processes that are involved in root soil
64 exploration, root nutrient acquisition and yield limitations as a consequence of both biotic and
65 abiotic interactions could enable new strategies for sustainable yield production through better
66 nutrient and water use efficiency, overcoming soil constraints and by improved C
67 sequestration (Kell, 2011, White et al., 2013b).

68 Roots have evolved to be extremely adaptable and responsive to their local environment.
69 Their growth, morphology and physiology are intimately linked to both the plant genotype
70 and the properties of the soil or medium in which they grow. For example, root elongation
71 rates and numbers of lateral roots can be reduced by high soil density or high water content

72 with a consequent reduction in shoot growth (Bengough et al., 2011, Bingham & Bengough,
73 2003, Grzesiak et al., 2002). Similarly, the availability of nutrients such as phosphate can
74 cause alterations in Root System Architecture (RSA) (Dai et al., 2012, Hammond & White,
75 2008, Lopez-Bucio et al., 2002) and root anatomy (Burton et al., 2013, Hu et al., 2014, Wu et
76 al., 2005). Ultimately, the abiotic stresses experienced by roots have an impact on the yield
77 of crops (Batey, 2009, Wang & Frei, 2011). In addition RSA and root growth are influenced
78 by biotic factors including saprotrophic and pathogenic micro and macro-organisms as well as
79 arbuscular mycorrhizal (AM) symbiotic associations (Osmont et al., 2007) and growth
80 promoting bacteria (Vacheron et al., 2013). Increased understanding of the plant responses to
81 both biotic and abiotic soil conditions may therefore assist in the selection of crop varieties
82 that are more resistant to invasion of plant pathogens (Bailey et al., 2006) or that are able to
83 take advantage of positive soil biotic interactions and may thus allow the selection of crops
84 that are pre-adapted to the impacts of climate change or particular abiotic soil conditions (Den
85 Herder et al., 2010).

86 Selection of crop varieties often involves the screening of large populations for specific
87 beneficial phenotypes in the search for quantitative trait loci that will enable the development
88 of genetic markers for marker-assisted breeding (Mir et al., 2012). Typically, these
89 populations range in size from 80 to 400 lines (Balasubramanian et al., 2009, Kreike et al.,
90 1996, Lebreton et al., 1995, Loudet et al., 2002, Quarrie et al., 1994, Ray et al., 1996),
91 however in the case of mutant populations the numbers can run into several thousands
92 (Bovina et al., 2014, Caldwell et al., 2004). These large populations and the need to
93 understand responses to variable environmental conditions, together with the highly variable
94 nature of root growth, leads to a requirement to phenotype several hundreds of individual
95 plants rapidly, under a range of environments or stress treatments with replication an
96 important consideration (Adu et al., 2014). In an ideal world, phenotyping of roots would be
97 achieved by time-lapse imaging of roots *in situ* in undisturbed soil in glasshouses or in the

98 field. Image analysis systems would be developed not only to record the shape of root
99 systems at a specific time point but also to provide information on the mechanisms of root
100 growth and the genetic or physiological responses over time. This would be linked to
101 information on the heterogeneous biological and physical environment of the soil.
102 Unfortunately, limitations to observations in soil are such that to be able to image living roots,
103 scientists must often find a compromise between growth conditions and quality of data
104 (Neumann et al., 2009).

105 Traditional methods for measuring roots grown in soil, such as root washing and root tracing
106 are destructive and slow (Smit, 2000). However, recent advances in imaging methodologies
107 including cameras, scanners, fluorescence and radiation based techniques, for example. X-ray
108 imaging, has enabled the non-destructive exploration of root growth processes and plant:soil
109 interactions with the abiotic and biotic environment, including soil pathogens and plant
110 growth promoting rhizobia (Abbas-Zadeh et al., 2010, Bao et al., 2014, Bengough et al., 2010,
111 Bloemberg et al., 2000, Downie et al., 2012, Keyes et al., 2013, Reddy et al., 2007, Valentine
112 et al., 2007, Wuyts et al., 2011). These various imaging techniques allow visualisation of
113 different aspects of soil structure, root growth and physiological processes, microbes and
114 water in soils or growth medium (Fig. 1). The majority of root measurements however are
115 still done *ex situ* by laying the roots on a flat surface, imaging them and later tracing them
116 (Clark et al., 2012, Clark et al., 2013, Hund et al., 2009, Villordon et al., 2011, Walter &
117 Schurr, 2005, Wells et al., 2012) and therefore, there is still a great deal of scope for
118 improving the collection of data on root:soil interactions using novel imaging and analysis
119 techniques.

120 Several recent reviews have detailed the progress in phenotyping root systems through
121 imaging and image analysis (Dhondt et al., 2013, Fiorani & Schurr, 2013, Zhu et al., 2011). In
122 this review we seek to establish that root phenotyping research must focus more on

123 interactions with environment and investigate rhizosphere traits and processes as well as root
124 phenotyping. This could be achieved by bringing together different imaging solutions, thus
125 linking the root phenotyping with quantification of rhizosphere processes. We first discuss
126 techniques for imaging and analysing roots and root growth dynamics. We also review
127 imaging and image analysis of roots within the context of delivering improved understanding
128 of root-genotype \times environment interactions (both abiotic and biotic) and give examples of
129 where combinations of technologies have allowed different aspects of the root:environment
130 processes to be explored. As part of this root:environment phenotyping process, scalable
131 methodologies, under conditions similar to those encountered in the environment, must be
132 developed that will allow knowledge to be translated to practical applications through
133 breeding programmes for new crop varieties. This will require pushing the boundaries of
134 both the imaging and computational techniques already available.

135 **PHENOTYPING ROOT SYSTEM ARCHITECTURE**

136 **2-Dimensional root imaging**

137 Root systems consist of numerous interconnected roots with different orders of lateral roots
138 and the RSA describes the system's morphology. Early studies of root systems date back to
139 the 18th century and mainly involved digging up roots and manually measuring their weight
140 and length. The ecologist J.E. Weaver (Weaver, 1919) (Fig. 2a) was one of the pioneers of
141 root research by field excavation, but many others also cultured plants in containers in order
142 to study their root systems (Bohn, 1979). Hiltner (1904), Bates (1937) and Kutschera (1960)
143 also quantified root systems in field soil or in pots by observation, sketching or tracing. Most
144 of these historic techniques including the measuring wheel, rulers or the transect methods
145 employed to determine the length of excavated washed roots were fraught with inaccuracies
146 and biases (Baldwin et al., 1971). More recently, attempts have been made to automate the

147 extraction process (Fig. 2b), (Benjamin & Nielsen, 2004) but fine roots are often lost during
148 these extraction processes. An alternative high throughput method was reported by Trachsel
149 et al. (2011) who carried out a high throughput screening study of root traits of mature plants
150 in the field, where many root traits from 218 inbred lines of maize were measured by shovel
151 excavation and visual scoring. The protocol is, however, destructive and laborious.

152 Recently the study of RSA has benefitted greatly from the introduction of relatively
153 inexpensive imaging facilities including flatbed scanners and digital video cameras (Ortiz-
154 Ribbing & Eastburn, 2003). Simple camera setups can be used to capture images of root
155 systems both *in situ* (Dannoura et al., 2012) and *ex situ* (Clark et al., 2011). Image acquisition
156 with these systems is technically simple, cheap, readily accessible, and can frequently offer
157 resolutions of up to 1600 dpi (scanners) or 8MP for cameras (Pierret et al., 2003). Scanners
158 and cameras facilitate high throughput experiments due to their image acquisition speed and
159 low cost (Dong et al., 2003). For example, Bengough et al. (2004) used flatbed scanner-based
160 2D gel chambers to predict which barley seedlings in landraces would develop shallow or
161 deep root distributions (Fig. 2c) and Shi et al. (2013) utilised a high throughput 2D growth
162 system and flat bed scanners to quantify root architectural traits enabling the identification of
163 QTL's associated with responses to Phosphate availability. 2D imaging is also suitable for
164 imaging roots growing in soil with flatbed scanner rhizotron systems (Dong et al., 2003).
165 These are often angled such that roots grow along the glass surface but are in contact with soil
166 (Dechamps et al., 2008). The advantage of the rhizotron system is that roots can be imaged
167 without disturbance and they have proved useful in assessing root growth dynamics in many
168 crops including apple trees, maize and barley as well as for studying the effects of changes in
169 water content during plant growth (Dong et al., 2003, Kuchenbuch & Ingram, 2002, Nagel et
170 al., 2012). The main disadvantage of 2D systems, such as flatbed scanners, is that they often
171 restrict root growth to a thin layer, which could potentially obscure the complex 3D
172 orientations of many root systems and could induce thigmotropic responses from the roots

173 due to the continuous root to glass contact. Further, most use plant culturing systems that do
174 not truly represent an undisturbed soil system in terms of mechanical impedance, temperature,
175 moisture distribution, solute concentrations and redox reactions (Herrera, 2012) and thus the
176 results obtained may not be applicable to field conditions (Bengough et al., 2004, Gregory et
177 al., 2009a, Gregory et al., 2009b, Watt et al., 2013, Wells et al., 2012, Wojciechowski et al.,
178 2009). Automated systems utilising scanners or cameras to take timelapse images of root
179 systems during development have recently been developed using either filter paper or soil
180 based systems (Fig. 2d, e), (Adu et al., 2014, Nagel et al., 2012). These systems generate
181 large datasets of images with their own individual image analysis challenges. These will be
182 discussed in detail later in this review.

183 Some phenotyping systems allow roots to grow in 3D space but also enable imaging of roots
184 in 2D. These include some aeroponics systems which produce roots that are more
185 anatomically similar to roots grown in soil than is achievable with hydroponics (Redjala et al.,
186 2011). These root systems are imaged using 2D acquisition tools, thereby losing information
187 on 3D root orientation. The data can nevertheless prove useful for high-throughput
188 phenotyping.

189

190 **3D root imaging**

191 At the cellular scale, 3D imaging of roots employs both destructive and non-destructive
192 methodologies. Imaging has utilised both fixed samples and transgenic plants expressing
193 fluorescent protein such as GFP to build 3D images (Bougourd et al., 2000). One destructive
194 method recently developed by Burton et al. (2012) for imaging root cellular structure uses
195 laser ablation of the root and gives a complex segmentable 3D image of the root cell structure.
196 Rapid screens such as this can be used to quantify the numbers of a particular cell type such
197 as aerenchyma that have been implicated in “cheaper” roots (i.e. ones that require a lower

198 resource input by the plant per produced length). This is potentially a beneficial phenotype in
199 drought regions where plants have to access deeper water resources (Lynch, 2013). This
200 latter method however is destructive.

201 There has also been a drive towards imaging roots *in situ* in 3D, through two separate
202 approaches, by either growing plants in soil and imaging using various forms of radiation
203 based imaging or through the development of artificial transparent growth media that allows
204 the visualisation of the root without disturbance using optical imaging, including confocal and
205 fluorescence based imaging (Fig. 2 f, Fig. 4h). Within this latter category, artificial media
206 have been developed for optical imaging of 3D RSA using plants grown in phytigel systems
207 (Fig. 2f) (Clark et al., 2011, Fang et al., 2011, Fang et al., 2009). Phytigel is similar to agar
208 and is homogeneous and water saturated. It is however, very dissimilar to common soils in
209 relation to soil strength, and therefore great care should be taken when interpreting the results
210 of experiments using different gel strengths to impose physical impedance on roots (Clark et
211 al., 1999). Recently, developments have been made to incorporate the physical heterogeneity
212 of soils into transparent substrates for culturing plants. This “Transparent Soil” (TS) made
213 from the particles of the ionic polymer (ionomer) Nafion allows control of moisture content
214 during plant growth in a granular, unsaturated substrate, thus allowing higher oxygen transfer
215 to the root system and interactions with a complex pore structure. To allow optical imaging
216 of roots, the substrate is saturated with a solution that is refractive index-matched to the
217 Nafion particles just prior to imaging (Fig. 4h) (Downie et al., 2012).

218 Both phytigel and TS can be used in combination with a number of imaging systems such as
219 Confocal Laser Scanning Microscopy (CLSM), Optical Projection Tomography (OPT) and
220 Light Sheet Microscopy (LSM) including the use of fluorescence to produce 3D images
221 (Downie et al., 2012, Yang et al., 2013). OPT is a 3D imaging system that can be used for
222 samples up to several millimetres in size and was developed for imaging animal embryos

223 (Sharpe et al., 2002). It has also been used to image plant shoots and roots (Lee et al., 2006).
224 The method involves projecting light through the sample and collecting transmission images
225 while the sample is rotated through 360°. Fluorescence can also be captured by using a UV
226 light source to illuminate the sample and emitted light can be captured as well as the
227 transmission images (Fisher et al., 2008).

228 Another useful recent development in microscope optics is the “mesolens” which is a lens 0.5
229 meters in length, with 4× magnification and a numerical aperture of 0.47 (Amos, 2010, Saini,
230 2012). It allows imaging of samples of up to 6 mm but with subcellular resolution without the
231 need to reconstruct the final image from a series of images. The developers aim to integrate it
232 into CLSM and light sheet microscopes for 3D imaging. The mesolens would allow the
233 imaging of the whole seedling root at high resolution, thereby, it would be potentially
234 possible to relate the root morphology and growth to cellular processes within one image
235 dataset.

236 Despite these advances in transparent growth media and optical imaging, 3D imaging in soil
237 remains central to root research. Soils have a great impact on root function and RSA
238 development (Wojciechowski et al., 2009) and there are still significant gaps in understanding
239 the reasons for the differences in plants grown in artificial systems vs soil grown plants.

240 Radiation tomography, such as X-ray tomography, Neutron tomography, Positron Emission
241 Tomography (PET) and Magnetic Resonance Imaging (MRI) have proven to be useful
242 methods to visualise roots in opaque growth media (Fig. 2g, Fig. 3g, Fig. 4c, Fig. 4d) (Asseng
243 et al., 1998, Jahnke et al., 2009, Moradi et al., 2009, Perret et al., 2007, Tracy et al., 2010,
244 Zappala et al., 2013).

245 Bois and Couchat (1983), Willatt and Struss (1979a), Willatt and Struss (1979b) and Willatt
246 et al. (1978) were pioneers in using radiation for studying roots and gained information about
247 germination time and root and shoot growth rates using neutron radiation. Medical scanners

248 were first used to visualize roots in soil and sand with X-ray tomography (Hainsworth &
249 Aylmore, 1983, Hamza et al., 2001, Hamza & Aylmore, 1992). The resolution that could be
250 achieved with medical scanners was $>1 \text{ mm}^3$ voxel size and therefore only coarse roots could
251 be detected. Higher resolutions were achieved using industrial scanners (Gregory et al., 2003,
252 Heeraman et al., 1997, Kaestner et al., 2006, Lontoc-Roy et al., 2006, Perret et al., 2007,
253 Tracy et al., 2010) and presently it is possible to achieve resolutions $<0.5 \text{ }\mu\text{m}$, with scanners
254 developed for material research (Tracy et al., 2010). The scan resolution is influenced by
255 sample size, focal spot size and detector. The highest resolutions can be obtained by X-ray
256 microtomography. In a recent study by Tracy et al. (2010) soil samples of 7 cm in height and
257 3 cm in diameter were scanned at a resolution of $24 \text{ }\mu\text{m}$, whereas resolutions obtained using
258 neutron tomography for similar sample sizes were $>50 \text{ }\mu\text{m}$ (Moradi et al., 2011). The
259 resolution that can be obtained with MRI is $>100 \text{ }\mu\text{m}$ (Segal et al., 2008). More recently,
260 images of root hairs in soil were obtained using synchrotron based X-ray tomography and
261 while the sample size at this resolution is at present extremely limited, the results were used to
262 enhance models of phosphate uptake by roots (Keyes et al., 2013) (Fig. 4g). The quality of
263 the images obtained with X-ray tomography can be adjusted with the number of angular
264 projections and the signal acquisition time per projection (Ketcham & Carlson, 2001). With
265 more angular projections images with less noise can be produced, but scanning duration will
266 be longer. For screening purposes it is important to keep the scan time as short as possible.
267 Although scanning times are rapidly improving, it may be some time before these are at
268 speeds sufficiently fast for screening purposes. This raises the question of whether screening
269 processes and analysis pipelines should be considered that comprise multiple methods.

270 **Towards imaging and image analysis of root system dynamics –**
271 **timelapse 2D and 3D imaging**

272 Root systems do not grow at the same rate throughout the lifecycle of the plant, therefore it is
273 important to understand both the process of growth and the lifecycle dynamics of root
274 systems. Water uptake and nutrient demand also depend on growth stage and season.
275 Imaging and quantification of root growth and functional dynamics has benefited greatly from
276 the introduction of time-lapse imaging but clearly this increases the quantity of data for
277 processing. Challenges for this area of research include the utilisation of computational
278 image analysis to increase accuracy, throughput and resolution (Baldwin et al., 1971). At the
279 acquisition stage, the length of time necessary to capture the image needs to be taken into
280 consideration particularly when dealing with 3D images. For analysis, high throughput but
281 accurate methods of extracting the relevant geometric features from the captured images must
282 be developed. Features of interest include RSA traits, such as root lengths, their relationships
283 (primary, seminal, 1st, 2ⁿ, 3rd etc order laterals), spatial distribution and cellular traits such as
284 root hairs and their dynamic behaviour. Simple techniques used to measure these traits have
285 been very informative. For example Darwin investigated root growth dynamics in crops
286 including *Brassica oleracea* and *Vicia faba*. By growing plants in wet sponges fastened to
287 transparent plates and manually tracing root growth with pencils he was able to reveal growth
288 dynamics such as circumnutation and geotropic root growth (Darwin, 1880, King, 1883).
289 Manual root sketches and traces are still useful, but not only are these methods painstakingly
290 time consuming they are also subjective. Root growth has also been captured using other
291 fairly simple imaging techniques, such as cameras and scanners (Adu et al., 2014, Clark et al.,
292 2013, Dannoura et al., 2012, Wells et al., 2012). For detailed studies involving the cells of
293 root tissues, magnification is required using microscopes. For example, CLSM and other
294 modern light microscopes connected to CCD camera can be software controlled to capture

295 time-lapse images of root growth (Bengough et al., 2010, van der Weele et al., 2003, Wuyts et
296 al., 2011).

297

298 Methods for the analysis of time-lapse images can be performed at an individual image level
299 using many of the methods described in the section above or by analysing the sequence of
300 images as an integral part of the analysis (Fig. 3). In the former, each individual image can be
301 analysed to study the cell structure or RSA at scales from confocal images showing root cell
302 structure through to 3D architecture, and then each individual structural description is joined
303 together to visualize the time-lapse dynamics of each quantified parameter (Fig. 3d, g) (Adu
304 et al., 2014, Federici et al., 2012, Galkovskyi et al., 2012, Zappala et al., 2013). Recently, an
305 interesting alternative approach has been taken by Basu and Pal (2012). They have
306 developed the concept of turning 2D time-lapse images into 3D topologies that describe the
307 changing root over-time (Fig. 3e). Alternative methods use more than one image for each
308 data “time-point” and the “motion” or “change between images” is analysed often using
309 optical flow algorithms. These techniques are more commonly used for cell growth or single
310 meristem analyses (Fig 3a, b). Beemster and Baskin (1998) and van der Weele et al. (2003)
311 (Fig. 3b), for example, studied living plants and analysed the relationship between root cell
312 division and expansion. Root gravitropic dynamics have also been studied using video
313 recording (Brooks et al., 2010, Mullen et al., 2000). The production of plants with a range of
314 spectral variants of fluorescent proteins marking cell membranes and nuclei has enabled
315 automated image analysis of the dynamics of root cells during root elongation of *Arabidopsis*,
316 using newly developed image analysis tools (Federici et al., 2012, Roberts et al., 2010, Wuyts
317 et al., 2011) (Fig. 3a). Functional information can be recorded through direct linking of
318 imaging, with image analysis and temporal expression of fluorescent markers linked to cell
319 development or physiological status of the root (Brady et al., 2007).

320 Time-lapse imaging and analysis in 3D has been limited partly due to the length of time it
321 takes to acquire 3D datasets. To reduce image acquisition time and light exposure of samples,
322 there has been a recent trend towards LSM techniques for 3D imaging of biological samples.
323 This technique uses a thin sheet of laser light which illuminates an optical section of the
324 sample. An objective lens is positioned at an orthogonal angle to the illumination plane and
325 the illuminated section of the sample is focused on. 3D images are created by moving the
326 sample through the illumination plane while a sequence of 2D images is captured (Huisken et
327 al., 2004). This technique has advantages over CLSM because of an improvement in the axial
328 resolution and also because the excitation light illuminates a much smaller section of the
329 sample for each image, thereby reducing potential problems of photodamage to the sample.
330 This is particularly important when imaging live specimens at multiple time points. Sena et al.
331 (2011) used light sheet fluorescence microscopy to image cell divisions and the nuclear
332 dynamics of *Arabidopsis* roots grown in a small hydroponics system over several days.
333 Similarly the *Arabidopsis* primary root tip growth and lateral root primordial growth has been
334 imaged using a light sheet based system (Maizel et al., 2011). These modern microscopes
335 improve acquisition speed, sample exposure and field of view, facilitating imaging over time
336 or studying large numbers of samples. In addition numerous research groups have custom-
337 built their own systems at relatively low cost to suit a particular application rather than relying
338 on commercially available systems (Clark et al., 2013, Clark et al., 2011, Huisken et al., 2004,
339 Santi et al., 2009, Sharpe et al., 2002).

340 At the root system scale, scanner banks, conveyors and standard cameras have been employed
341 to generate high throughput and time-lapse datasets (Adu et al., 2014, French et al., 2009,
342 French et al., 2012). For example a high throughput 2D system of two cameras fixed to a
343 conveyor was used to image root systems of up to 20 genotypes of *Arabidopsis* plants and the
344 images were analysed automatically using customised software to extract quantitative
345 information about root growth dynamics (Fig. 3c) (French et al., 2009, French et al., 2012).

346 Similarly, (Nagel et al., 2012) described a prototype for automatically analysing RSA in 2D
347 for plants grown in rhizotrons (Fig. 2d). This system has increased throughput, allowing
348 simultaneous camera imaging of root and shoot growth from up to 72 rhizotrons per hour.
349 The utilisation of X-ray CT imaging for time-lapse growth studies has also been restricted,
350 partially due to the length of time required for each image scan. However, recent reductions
351 in scan time to less than 20 minutes while maintaining the necessary resolution for
352 segmentation of roots from the collected images has allowed Tracy et al. (2012a), Tracy et al.
353 (2012b) and Zappala et al. (2013) to compare root growth and development in 3D images of
354 tomato plants and rice imaged over 9 consecutive days and to compare the roots of 3 varieties
355 of wheat by rescanning seedlings at 2, 5 and 12 days after germination (Fig. 3g). Despite the
356 decrease in scan time, timelapse - X-ray CT is still limited to tens rather than hundreds of
357 scans per day.

358 Combinations of techniques can also reveal functional processes within plant roots using
359 time-lapse imaging. This include methodologies such and PET and MRI, where, for example,
360 carbon allocation can be tracked by following tracer molecules using PET, placed in a plant
361 context by imaging of the plant structure using MRI (Fig. 3f). These combined
362 methodologies may also prove useful in understanding the root:rhizosphere interactions.

363

364 **IMAGING ROOT:RHIZOSPHERE INTERACTIONS**

365 The soil environment and the rhizosphere significantly influence the overall shape and size of
366 root systems. Roots can also influence each other, affecting root growth, lateral root
367 production and, ultimately, root architecture. Utilisation of fluorescence technology has
368 started to allow us to separate the different influences on root growth through labelling of

369 roots to separate individual plants (Faget et al., 2013, Faget et al., 2009, Faget, 2013) , and
370 labelling of roots and rhizosphere bacteria and fungi to study colonisation (Downie et al., 2012,
371 Downie et al., 2014, Gage et al., 1996, Genre & Bonfante, 2005). Further, the physiological
372 responses of plant roots to their environment can be visualised utilising the multitude of
373 reporter proteins now becoming available (Chapman et al., 2005, Dixit et al., 2006, Okumoto
374 et al., 2012). One of the major advances of non-destructive imaging of root systems is that it
375 offers opportunities to quantify root interactions with the biotic and abiotic environment.

376 **Interactions with Biota**

377 There is growing evidence to indicate that the microbiome associated with plants roots is
378 highly important for plant health, where the plant is able to shape the community of
379 microorganisms it associates with, for example, by recruiting bacteria which can protect it
380 from pathogens (Berendsen et al., 2012). Soil microorganisms can have a significant effect
381 on root growth both indirectly due to nutrient turnover but also directly due to mechanisms
382 such as nodulation, perception of bacterial quorum sensing signals or the production of plant
383 hormones such as auxin by the bacterial population (Bauer & Mathesius, 2004, Goh et al.,
384 2013). The interaction between soil biota and roots is of interest for a number of applications
385 including biological pest and disease control, plant growth promotion through enhanced
386 nutrient supply from bacterial processes and rhizoremediation to improve soil quality. A
387 greater understanding of these complex interactions could lead to new opportunities for
388 protecting plants from diseases whilst limiting the use of agrochemical control products
389 (Chaparro et al., 2012). Imaging and image analysis of thin embedded sections of soil cores
390 have revealed soil stabilisation processes involving roots and bacteria (Bruand et al., 1996).
391 Fluorescence *in situ* hybridisation (FISH) can also be carried out on soil samples in order to
392 label microorganisms so that they can be detected using microscopy techniques after
393 sectioning the soil sample (Eickhorst & Tippkoetter, 2008, Moter & Gobel, 2000). Further,

394 FISH has been used to detect and quantify bacteria colonising wheat roots after extraction of
395 the roots from soil (Watt et al., 2006). However, while there has been a great development in
396 imaging techniques to visualise roots in 3D *in situ* in soil, resolution currently limits the direct
397 visualisation of bacteria and individual fungal hyphae in soil. In contrast, utilisation of
398 fluorescent reporter proteins such as GFP expressed by fungi and bacteria (e.g., *Fusarium*
399 *oxysporum*, *Pseudomonas fluorescens* and *E. coli*) has enabled the exploration of root
400 colonisation by bacteria in 2D or 3D, gel or TS media (Fig. 4a) (Czymmek et al., 2007,
401 Downie et al., 2012, Downie et al., 2014, Gamalero et al., 2005, Humphris et al., 2005,
402 Martino et al., 2007, Nonomura et al., 2003). Similarly, Haynes et al. (2004) developed a
403 system for observing different stages of nodule formations in legumes. This enabled rapid
404 screening and isolation of plant nodulation mutants with phenotypic differences in thread
405 growth and cellular invasion. Recently, the TS system was used to quantify bacterial
406 distribution after imaging bacteria and roots live and *in situ* (Downie et al., 2014). Similarly
407 CLSM imaging has been used to study the interactions of viruses and parasitic nematodes
408 with plant roots *in situ*, *in vitro* (Fig. 4b) (Valentine et al. (2004), Valentine et al. (2007)) and
409 developments in plant growth substrates such as TS may facilitate a better understanding of
410 how root morphology impacts biotic interactions (Downie et al., 2012, Downie et al., 2014).
411 While in many of these studies the fluorescent tag is used as a tool for imaging where the
412 roots or bacteria or viruses are present, the development of dynamic reporters has also
413 enabled the exploration of the dynamic communications and interactive processes such as
414 bacterial responses to specific plant exudates via utilisation of LUX reporters or fast folding
415 forms of GFP-based fluorescent proteins (Rochat et al., 2010).

416 In soil, X-ray microtomography has also been useful to help understand macrobiotic
417 interactions with roots as it was used to track the movements of the pest *Sitona lepidus* larva
418 towards clover roots nodules (Fig. 4c) (Johnson et al., 2004). For many of these areas of
419 study, the challenge is now to increase the throughput of these techniques, to extend and

420 enable high throughput screening by automation of the techniques, and also to enable the use
421 of 3D and 4D (3D x time) imaging of processes where appropriate.

422 **Interactions with abiotic aspects of soil**

423 Changes in soil pH, water content, oxygen availability, strength, macropore availability, bulk
424 density, aggregate size and root:soil contact can affect root elongation and impact on water
425 and nutrient uptake rates of roots (Schmidt et al., 2012, Tracy et al., 2012a, Tracy et al., 2013,
426 Tracy et al., 2012b, Valentine et al., 2012b, Veen et al., 1992). Further, roots forage for
427 nutrient in variable nutrient patches within the soil while elemental toxicity and effects such
428 as salinity can cause significant changes in root elongation rates and architecture (White et al.,
429 2013a, White et al., 2013b). Equally, as roots penetrate through the soil they influence the
430 physical and chemical structure and composition around them (Czarnes et al., 2000, Lambers
431 et al., 2009). Our limited understanding of how roots can overcome and adapt to abiotic
432 conditions is potentially one of the major limitations in translating results from laboratory and
433 glasshouse studies of root behaviour to field conditions (Bengough et al., 2004, Gregory et al.,
434 2009a, Valentine et al., 2012b). Field soil is far more physically heterogeneous than
435 laboratory conditions and roots can exploiting the high variability in soil strength, soil pore
436 structure including biopores and macropores and water availability (Bengough et al., 2011,
437 Ehlers et al., 1983, McKenzie et al., 2009, Valentine et al., 2012b, White & Kirkegaard, 2010).

438 Recently, time-lapse, CLSM, X-ray CT and Neutron radiography techniques have all been
439 used to explore the relationship of roots with their physical environment. Bengough et al.
440 (2010) grew *Arabidopsis* plants in a mixture of gel and glass ballotini and imaged the growing
441 roots using CLSM. Using Particle Image Velocimetry (PIV) they showed root growth
442 kinematics at the cell and meristem scale and additionally quantified the displacement of the
443 external granular media (Fig. 4f). The root cap and mucilage had a considerable impact on
444 this interaction for maize seedlings in sand (Vollsnæs et al., 2010). Application of this type of

445 analysis to root growth and dynamics of the environment is limited currently by the
446 requirement to obtain data with the right resolution and within short time scales. The TS in
447 combination with optical tomography (Downie et al., 2012) is also a suitable system for this
448 type of research due to the particulate nature of the medium and the ability to control the
449 substrate particle size as well as the water content. In real soil systems, X-ray tomography is
450 especially suited to imaging the soil structure and its relationship with root architecture. Using
451 X-ray CT, Tracy et al. (2012a) and Tracy et al. (2012b) showed that effects of bulk density on
452 root growth were in agreement with destructive studies, and they were able to quantify the
453 decrease in root length with increasing bulk density. Perhaps more striking, and not
454 achievable with other destructive methods mentioned previously, a method for estimating
455 root:soil contact from 3D volumetric images (X-ray-CT) was developed by Schmidt et al.
456 (2012) and the effects of growth material and matric potential on root:soil contact and root
457 elongation rate has been investigated (Fig. 4e). Root:soil contact dynamics from 3D
458 microtomographs were also studied by Carminati and Fluehler (2009) by determining the gap
459 around roots after wetting and drying cycles, but actual root:soil contact was not quantified.
460 High resolution imaging has also allowed the visualisation of the interaction of root hairs and
461 particles in artificial media (TS) and soil (Downie et al., 2012, Keyes et al., 2013) (Fig. 4g,h).
462 Root hairs are important features involved in the soil contact, are affected by the soil physical
463 and chemical conditions and are integral to the development of potentially important
464 agricultural traits such as the rhizosheath (Brown et al., 2012, Delhaize et al., 2012, George et
465 al., 2014, Haling et al., 2014, Watt et al., 1993). Root hairs, root:soil contact and rhizosheath
466 development are thus important parameters in understanding uptake of water and nutrients by
467 roots and the ability to image these and follow changes dynamically will be a huge step
468 forward in understanding root function.

469 In addition to the soil-structure relationships discussed above, the spatial distribution of water
470 around roots has been a topic of extensive investigation with 3D imaging techniques

471 (Bottomley et al., 1986, Carminati et al., 2010, Hamza et al., 2001, Hamza & Aylmore, 1992,
472 Macfall et al., 1990, Macfall et al., 1991, Moradi et al., 2011, Oswald et al., 2008, Pohlmeier
473 et al., 2008, Segal et al., 2008, Tumlinson et al., 2008). Using a whole body X-ray CT
474 system, Grose et al. (1996) showed how wheat seedlings were surrounded by a heterogeneous
475 landscape of water content and derived from that their susceptibility to infection. As root
476 material and soil water solution show similar attenuation coefficients, contrast enhancers are
477 often used before the water content can be determined from changes in greyscale values
478 (Carminati *et al.*, 2009, Hainsworth & Aylmore, 1983, Wildenschild, Hopmans, Rivers &
479 Kent, 2005). MRI and Neutron radiography are, in contrast, very sensitive to changes in
480 water content due to the interaction with H-atoms. Studies using MRI, to measure water
481 uptake and dynamics around individual roots showed that fine roots of loblolly pine (*Pinus*
482 *taeda* L.) were more efficient than tap or lateral roots at water uptake (based on weight)
483 (Macfall et al., 1990, Pohlmeier et al., 2008, Segal et al., 2008). In more recent studies,
484 neutron radiation has been used to visualize and quantify water distribution in close proximity
485 of roots in 3D (Carminati et al., 2010, Moradi et al., 2011, Oswald et al., 2008). It is worth
486 noting that these techniques are limited in their application to soils of intermediate water
487 content and with a content of ferromagnetic particles <4%, as both high and low water
488 content can lead to low contrast and ferromagnetic particles cause artefacts (Bottomley et al.,
489 1986, Macfall et al., 1990, Macfall et al., 1991, Pohlmeier et al., 2008, Rogers & Bottomley,
490 1987).

491 Of the chemical characteristics of the root:soil environment, pH has received the most
492 attention. Most recently, rhizosphere pH has been explored using videodensometry and planar
493 optode imaging (Blossfeld & Gansert, 2007, Blossfeld et al., 2010, Blossfeld et al., 2013,
494 Rudolph et al., 2012, Rudolph et al., 2013). This technique allows for detailed, dynamic 2D
495 imaging of pH gradients with the plants growing in soil and the roots growing along a flat
496 surface with a planar optode. By imaging roots at 15-minute intervals, daily variations in pH

497 and overall acidification were revealed. The application of optodes is not limited to studying
498 pH. For example, Blossfeld et al. (2011), Blossfeld et al. (2013) and Rudolph et al. (2012)
499 carried out studies on the dynamics of rhizosphere pH and soil oxygen and CO₂ which have
500 important implications in the survival of rhizosphere bacteria and rates of inhibition of root
501 growth due to hypoxia (Fig. 4d). The technique has also been used to study the depletion of
502 ammonium around roots (Stromberg, 2008) and in bulk soil (Delin & Stromberg, 2011).
503 Further dissolved P distribution and depletion zones around roots have been imaged by
504 Santner et al. (2012), using diffusive gradient films and laser-ablation inductively coupled
505 plasma mass spectrometry. These techniques currently applicable to 2D imaging can be
506 combined with techniques such as neutron imaging to investigate the integral links between
507 plant architecture and the chemical dynamics. The quantification of rhizosphere processes
508 made possible with these techniques, make it likely that these adaptable approaches will
509 become more popular and available to root researchers as an imaging tool in the future.

510 **RESOURCES FOR IMAGE ANALYSIS.**

511 There are a growing number of resources for image analysis available and these have recently
512 been assembled in an online database that can be found at www.plant-image-analysis.org
513 (Lobet et al., 2013). Computed image analysis encompasses a cascade of processes including
514 image acquisition, enhancement, storage and quantification (Duncan & Ayache, 2000).
515 Image analysis of roots frequently involves digitally separating or segmenting them from non-
516 root objects within the image and is often fundamental and challenging (Zhang et al., 2008).
517 Utilising transparent growing systems (e.g. gels and TS) along with fluorescent markers or
518 stains can facilitate the image segmentation during root functional studies (Downie et al.,
519 2012, Faget, 2013, Federici et al., 2012, Wuyts et al., 2011). However, root images, 2D or 3D,
520 colorimetric or grayscale, often include artefacts that complicate the processing and extraction

521 of information (Lobet et al., 2011). While developments in computer capabilities mean that
522 segmentation of digital images could be automated and accelerated, there is no off the shelf
523 solution for all data sets (Sezgin & Sankur, 2004). Different images require different
524 segmentation procedures resulting in potential subjectivity (Zhang et al., 2008).

525 Software dedicated to root system analysis should be capable of discriminating roots from
526 non-roots based on simple shape descriptors other than pixel or voxel intensity gradients
527 alone. When imaging in soil using X-ray scanners, some soil particles, water and roots have
528 overlapping distributions in the histograms of image intensity. These cause problems in
529 segmenting the different phases of the sample (Mairhofer et al., 2012, Tracy et al., 2010).

530 Recently, Mooney et al. (2012) summarised in detail the developments in image segmentation
531 when studying roots. Two approaches have primarily been used: separation of the image parts
532 by their position on a histogram of the entire image (i.e. clustering by global thresholding) or
533 identifying a region by growing the region of interest from a seed point (i.e. co-opting parts of
534 the image around an initial seed point depending on its value relative to a local threshold)
535 (Gregory et al., 2003, Mooney et al., 2012, Pierret et al., 1999a, Pierret et al., 1999b). The
536 global threshold can overestimate the root volume by 10 fold (Mairhofer et al., 2012).

537 RootViz3D® and Roottrak, have been developed from these segmentation techniques using
538 automated tracking approaches (Jassogne et al., 2009, Kaestner et al., 2006, Mairhofer et al.,
539 2012, Perret et al., 2007, Tracy et al., 2010). Segmentation of roots in RootViz3D® is based
540 on applying a probability function to determine whether a specific voxel represents root
541 material. Roottrak employs multiple models of the appearance of root material, where models
542 built from root sections are identified and used to search for root material in another section
543 (Mairhofer et al., 2011). RootViz3D overestimated segmented root volumes compared with
544 data obtained on washed roots using WinRHIZO® (Tracy et al., 2012a). Improvements in
545 segmentation techniques for roots over the past 15 years have reduced the error in root length
546 and volume measurements from between 21% and 42% (Heeraman et al., 1997) to 10%

547 (Gregory et al., 2003, Perret et al., 2007). This error is expected to be reduced further with
548 developments in scanning resolution and segmentation algorithms.

549 Root research would also benefit from a greater integration of the numerous existing
550 algorithms employed in clinical image analysis. Objects such as vascular networks or neural
551 network share many similarities with root systems in their intricacies, complexities and
552 structure. Accordingly, the integration of pre-processing algorithms common in medical
553 image analyses such as vesselness, hessian-based filters and livewire segmentation into root
554 image analysis programs could be applicable (Frangi et al., 1998, Poon et al., 2007) . These
555 shape descriptor-based filters are capable of searching for geometrical structures which can be
556 regarded as tubular and would be less affected by the presence of noises of different shape
557 orientations. For example, livewire-assisted semiautomatic segmentation was recently
558 employed to analyse root growth dynamics of *Phaseolus vulgaris* and *Cicer arietinum* from
559 2D time series images, from which spatio-temporal 3D structures were constructed to reveal
560 multimodal transient growth zone in basal roots (Basu & Pal, 2012).

561 Recently there has been a trend in root system analysis software to facilitate the quantification
562 of traits more complex than number and lengths of root axes, lateral root length and density,
563 which are most commonly measured (Draye et al., 2010, Dubrovsky & Forde, 2012).

564 Analysing images of roots in soil from rhizotron and minirhizotron systems can be more
565 complicated (Neumann et al., 2009, Wells et al., 2012). Gasch et al. (2011) proposed the use
566 of geographic information systems (GIS)-based image analysis technology for these types of
567 images where the operator selects a few target features within an image to serve as “learning
568 sets” to train the software in locating additional similar features within the image. Once
569 validated, the feature analyst approach of classifying pixels based on spectral characteristics
570 could enhance rhizotron image analysis.

571

572 **LIMITATIONS**

573 Efforts are increasingly being made throughout the scientific community to develop solutions
574 to some of the current limitations in imaging root systems (Dhondt et al., 2013, Fiorani &
575 Schurr, 2013, Mooney et al., 2012) . Each of the imaging and analysis systems described
576 above has advantages and disadvantages. While fluorescence techniques for example, can
577 offer real-time gene expression analysis, X-ray and MRI offer root images *in situ* in soil and
578 PET offers metabolite tracing. It is possible that a greater level of understanding could be
579 gained from addressing some of the limitations, and where possible, combining
580 methodologies. Recently for example, staining techniques have been developed in animal
581 research that allow protein expression patterns to be visualised using μ CT (Metscher &
582 Mueller, 2011) and efforts are also being made to combine different methodologies
583 harnessing the power of each. Jahnke et al. (2009) have combined PET and MRI imaging to
584 track the allocation of C over time in sugar beet tubers (Fig. 2f) , radish and maize roots, the
585 latter of which were imaged *in situ* in soil over time. Since several short and long-lived
586 positron emitting radiotracers are becoming available for tracing a variety of metabolites and
587 some elements (Ishikawa et al., 2011, Kiser et al., 2008), there is much scope for further
588 developments in this area. Rhizosphere interactions are also accessible to this combined
589 approach. Faget et al. (2013) have combined the use of planar optodes to measure soil pH
590 dynamics with GFP expressing plants to differentiate root identity in soil, enabling
591 examination of the different species interactions and the effect of this interaction on soil
592 acidification. Rhizopshere microbial and root phosphatase co activity have also been mapped
593 using soil zymography and ^{14}C imaging revealing spatial differentiation of activity and
594 activity groups (Spohn & Kuzyakov, 2013). These few examples show the potential gains
595 obtainable by combining the power of different methodologies to understand not only the

596 behaviour of plants but also in some cases to gain an understanding of the influence of the
597 rhizosphere on the processes studied.

598 To increase throughput, many systems are employing robotics and conveyor belts to move
599 plants automatically and position them in front of the imaging devices (see examples Table 1).
600 Many, however, are limited by their proprietary software, complexity and large investments
601 needed for their infrastructure. The cost of imaging technologies is therefore a major barrier
602 to broad availability and in addition to the “high investment” phenotyping systems there is a
603 need to develop root imaging technologies and applications that are cost-effective and thus
604 are readily accessible (Tsaftaris & Noutsos, 2009). Cheaper systems may also have the benefit
605 of replication and high throughput (Reynolds et al., 2012); recent examples include Adu et al.
606 (2014). Cheaper high-throughput root phenotyping will also aid reverse genetic approaches,
607 where the screening of many genotypes is needed (Walter et al., 2012). Some of the
608 boundaries of cost of access to high-cost facilities are being overcome by initiatives such as
609 the IPPN (International Plant Phenotyping Network www.plant-phenotyping.org) and EPPN
610 (European Plant Phenotyping Network www.plant-phenotyping-network.eu) which can assist
611 in making the larger automated platforms available for researchers around the globe.
612 Examples of some of the automated systems focused on roots are included in Table 1. These
613 initiatives also bring together experts in the different phenotyping technologies, so have the
614 potential to facilitate combinations of techniques.

615 Currently, there are severe limitations in the size of samples which can be imaged (Herrera et
616 al., 2012). For many 2D imaging systems, plant growth is restricted to the seedling stage due
617 to the size of rhizoboxes, making translation of results to mature plants challenging. 3D
618 images from gel and TS samples published so far mostly range in the region of less than 5cm
619 diameter, and the most common volume of X-ray CT images are also in the region of 5 cm
620 diameter (Downie et al., 2012, Lind et al., 2014, Tracy et al., 2010). Some of the recently

621 developed systems are pushing the sample size boundaries: with some automated systems
622 using 18L soil volume, and allowing a root depth of 90 cm (Nagel et al., 2012). The system
623 at the University of Nottingham will facilitate phenotyping roots in samples with soil volumes
624 of 30 cm x 100 cm (<http://www.cpib.ac.uk>).

625 Development of field-based imaging systems is also essential for validation of data obtained
626 from laboratory based experiments. With adequate development in terms of throughput,
627 applicability to all soil types and to crop plants of varying developmental stages, geophysical
628 imaging techniques hold potential in field-based root and rhizosphere research (Luster et al.,
629 2009). Ultimately, the target is to achieve high-throughput screening of root traits under field
630 conditions but most current soil and field-based methods including soil cores (Herrera, 2012)
631 and computed tomography methods (Tracy et al., 2010) are yet to realize this objective.

632 Geophysical methods including electrical resistivity, capacitance and ground penetrating
633 radar (Amato et al., 2009, Barton & Montagu, 2004) could offer fast and automated field
634 measurements, but care must be taken to validate methods as accurate root detection has not
635 been achieved so far. (Dietrich et al., 2013). Geophysical methods can be 2D or 3D, and have
636 been used to produce images of root systems *in situ* in the field using information on soil
637 moisture distribution (al Hagrey, 2007), and there is also the potential to monitor changes and
638 processes in 4D.

639 Further development in phenotyping must consider the implications of using commercial vs
640 homemade systems. While commercial systems come with full pre-testing, which may put
641 them at an advantage over a homemade systems, many homemade systems are built on open
642 source software and are therefore cheaper and potentially more easily manipulated for
643 specific situations. Progress in the development of robust and faster computer hardware and
644 software for image analysis must be concurrent with proper experimental designs and
645 statistical power of analyses. Further, mathematical modelling approaches should be integral

646 in analysing resulting data in order to reveal temporal and spatial variation that might be
647 inherent in the data as a result of local environmental effects. Moreover, for optimal
648 exploitation of emergent and scaled-up phenotyping approaches, it is imperative that suitable
649 databases and bioinformatics tools are developed to manage the large, complex datasets.
650 Central databases and automated management of data flows and retrieval will aid cross-
651 laboratory communication and lead to the creation of a powerful knowledge environment for
652 linking genotype-phenotype root system information (Thorisson et al., 2009). The possibility
653 of combining or creating a universal platform that integrates multiple platforms will represent,
654 potentially, a tremendous breakthrough. Hapca et al. (2011) have developed a method of
655 sequential sectioning to align 2D chemical maps with 3D volumetric images. This method
656 offers the potential to link information obtained with 2D image techniques to spatial data
657 obtained with radiation techniques that can operate in 3D such as combining X-ray
658 tomography and positron emission tomography (PET) to study changes in soil chemistry and
659 assimilate allocation in the rhizosphere (Garbout et al., 2012, Jahnke et al., 2009). Further
660 progress is also likely to be made by combining synchrotron techniques with both modelling
661 and plant molecular biology (Donner et al., 2012, Keyes et al., 2013)

662 **SUMMARY AND FUTURE DIRECTIONS**

663 Generating robust, reliable and relevant root and rhizosphere trait information is the key to
664 understanding root:soil interactions and to ensure enhanced and sustainable crop production
665 in a changing climate. Currently, selection and breeding of crop genotypes based on root traits
666 is extremely limited. Variability and stochasticity of root traits is such that the number of
667 replicates required to detect differences is very high. It is made more challenging by the high
668 Genotype x Environmental interactions that are implicit in root plasticity. The need to
669 incorporate the diversity of soil in which crops are grown, the strong heterogeneity of soil

670 conditions, and the biotic and abiotic interactions, adds a further level of complexity.
671 Optimisation of statistical power of collected data must therefore be considered in order to
672 provide reliable estimates of phenotypes and G x E effects (Walter et al., 2012). For root
673 imaging to make an impact in agriculture, it will have to enable detailed analysis of root
674 systems and rhizosphere status at spatial and temporal scales that have not been achieved
675 before (Houle et al., 2010). Increasing pixel or voxel resolution and faster image acquisition
676 techniques and time-lapse studies have greatly increased the amount of image data available
677 for root analyses. The present need for high throughput screening and data aggregation across
678 many different sites for genetic and QTL studies will further compound issues of image
679 capture, image processing speed and complexities of the image analysis process. However,
680 efforts are being made to produce more integrated and high-throughput systems (Armengaud
681 et al., 2009, Wells et al., 2012).

682 There is the possibility to link genetics to our understanding of both root growth and
683 physiological processes. Recent increased resolution of radiation based techniques and
684 developments in optical techniques such as fluorescence OPT, LSM and the mesolens allow
685 analysis of larger samples and give significant scale overlap between the methodologies.
686 Each technique has advantages in visualisation of specific processes and specific imaging and
687 analysis methods are required to extract the biologically relevant information. Table 2
688 summarises the root:soil processes that have been examined using the different imaging
689 techniques. Imaging techniques to study roots and soil have proven to be useful tools to gain
690 knowledge about root architecture, water transport and uptake, effects of soil structure on root
691 growth, root:soil contact and interactions with the biotic environment but it is important to
692 consider the choices in methodology at all stages of the imaging pipeline. Figure 5 illustrates
693 several options to be considered at each stage of the phenotyping pipeline, such as size of
694 sample or growth substrate. Many of the variables will affect the image analysis process and
695 the ability to automatically extract the root:rhizosphere traits from the images later in the

696 phenotyping process (Fig. 5). We can now: (i) image and quantify root and rhizosphere
697 dynamics over time; (ii) obtain data on density and clustering of roots and link this with plant
698 nutrient uptake and biological interactions; (iii) establish links between root hierarchy and age
699 and response to environmental stimuli; (iv) demonstrate interactions with the environment,
700 both local and global; and (iv) integrate understanding of the effect of the environment over
701 time and space. Due to the reduction in cost of many imaging technologies, and the
702 development of new analytical algorithms and hardware with increased computation power, it
703 is now possible and beneficial to combine or link the different system to gain an integrated
704 understanding of root growth, root physiology and rhizosphere interactions using the benefits
705 of the different systems.

706 **ACKNOWLEDGEMENTS**

707 This work was funded via the Scottish Government RESAS research programme,
708 Distinguished Scientist Fellowship Program, King Saud University, Riyadh, Saudi Arabia
709 (Prof White) and postgraduate studentships funded via the James Hutton Joint Studentship
710 scheme, Prof. Malcolm Bennett Professorial fellowship and Abertay University. We would
711 also like to thank Prof. Malcolm Bennett, Prof. Martin Broadley and Dr. Tim George for
712 helpful comments on the manuscript.

713 **TABLES**

714

715

716

Table 1: Root Phenotyping facilities

718

Location	Facility	Link	719
			720
The James Hutton Institute	Scanner bank	http://www.archiroot.org.uk	721
Aberystwyth University	Plant Phenomics Centre	http://www.phenomics.org.uk/	
University of Nottingham	X-ray Computed Tomography (μ CT)	http://www.cpib.ac.uk	
The Australian Plant Phenomics	The Plant Accelerator®	http://www.plantaccelerator.org.au/	
Jülich , Germany	Jülich Plant Phenotyping Centre	http://www.fz-juelich.de/	
Montpellier, France		http://www.montpellier.inra.fr/	
LemnaTec		http://www.lemnatec.com	

Table 2: Applicability of imaging techniques to root:rhizosphere interactions (x low usage to xxx highly suitable)

	X-ray tomography	MRI	Neutron tomography	PET	Optodes	Flat bed scanners	Cameras	Fluorescence microscopes	CLSM	Light-sheet microscopes	OPT
Soil structure (2D)	xxx	xx	-	-	x	x	x	x	x	-	-
Soil structure (3D)	xxx	x	-	-		-	-	-	-	-	-
Root system architecture	xxx	x	x	-		xxx	xxx	x	-	x	xxx
Root cellular structure	-	-	-	-		-	-	xxx	xxx	xxx	-
Root cellular processes	-	-	-	-		-	-	x	xxx	xxx	-
Root - microbe interactions	-	-	-	-	x	-	x	x	xxx	xxx	x
Water	x	xxx	xxx	-		-	-	-	-	-	-
Chemicals	-	-	-	xxx	xxx	xxx	x	x	xxx	x	x

723 **FIGURE LEGENDS**

724 **Figure 1. Visualisation of rhizosphere abiotic and biotic interactions**

725 Interactions at the rhizosphere involve many different physical, chemical and biotic processes.
726 This requires a range of imaging and image analysis solutions. Soil chemistry images courtesy
727 of Simona Hapca. Microbes, (left) Downie et al. (2012), (right) with kind permission of
728 Elsevier Limited, reproduced from Harris et al. (2002).

729

730 **Figure 2. Root imaging from destructive harvests to 2D automated** 731 **imaging systems and 3D phenotyping**

732 Root imaging from destructive harvests to 2D automated imaging systems and 3D
733 phenotyping of roots in soil. Imaging systems have progressed from manual tracing of roots
734 extracted from soil through to *in situ* analysis of roots growing in soil. Root were initially
735 manually extracted from soil and an image produced by tracing the roots (a). Some
736 automated systems for extracting root from soil have been developed (b). Scanners can be
737 used to assist in analysis and quantification of extracted roots or for capturing of root data *in*
738 *situ* in both gel and soil systems (c, d, e). These scanner systems are conducive to automated
739 image capture of root growth of multiple plants due to either multiple scanning points (e) or
740 by automated movement of plant growth boxes (d). 3D analysis of roots growing in gels
741 systems for optical imaging or in soil using for example, x-ray- μ Ct imaging is also possible (f,
742 g)

743 (a) Manually traced root systems (Weaver, 1919) . (b) Automated extraction of roots from
744 soil (Benjamin & Nielsen, 2004) . (c) Barley seedlings grown in 2D soil and gel system
745 imaged by scanner illustrating root growth patterns (Bengough et al., 2004). (d) Automated

746 robotic phenotyping system, GROWSCREEN-Rhizo (Nagel et al., 2012). (e) Multiple
747 automated scanner bank for automated time-lapse imaging of roots growing on filter paper
748 (Adu et al., 2014). (f) Roots growing in a gel based system used for 3D tomography optical
749 imaging (Clark et al., 2011). (g) Roots in situ in soil imaged using x-ray- μ Ct (Zappala et al.,
750 2013). (a) Reproduced under open licence from DigitalCommons@University of Nebraska.
751 (b, c, g) Reproduced with kind permission from Springer Science and Business media. (d)
752 Reproduced with kind permission from CSIRO Publishing. (f) Reproduced with kind
753 permission from the American Society of Plant Biologists.

754 **Figure 3. Analysis of Root system architecture dynamics**

755 Analysis of root growth dynamics from cellular through to architectural scale using motion
756 analysis (a, b) or time-lapse snap shots (c-g). (a) Motion analysis of individual cell
757 boundaries to analyse cell expansion utilising *PlantVis-R* (*Arabidopsis* expressing GFP:LTI
758 in the plasma membrane imaged using CLSM) (Wuyts et al., 2011). (b) Kinetic analysis of
759 root elongation at the meristem scale using IR imaging (van der Weele et al., 2003). (c)
760 Automated camera based high-throughput imaging and image analysis of root elongation and
761 curvature (French et al., 2009). (d) Automated scanner bank (see Figure 2e) based
762 architectural analysis (previously unpublished image, (Adu et al., 2014). (e) 3D visualisation
763 of root architecture changes over time (Basu & Pal, 2012). (f) Analysis of C sequestration
764 using a combination of MRI and PET imaging (Jahnke et al., 2009). (g) Repeated imaging of
765 Rice roots in situ in soil using X-ray μ -CT imaging (Zappala et al., 2013) allowing analysis of
766 3D architectural dynamics in soil.

767 (a, g) Reproduced with kind permission from Springer Science and Business media. (b, c)
768 Reproduced with kind permission from the American Society of Plant Biologists. (d)
769 Previously unpublished image (e, f) Reproduced with kind permission from John Wiley &
770 Sons.

771

772 **Figure 4. Imaging and image analysis of biotic and abiotic interactions**
773 **at the root:rhizosphere interface**

774 Imaging and image analysis of biotic and abiotic interactions at the root:rhizosphere interface.
775 Visualisation of biotic interactions (a-c), chemical (d) and physical interactions (e-h). (a)
776 GFP expressing bacterial colonies forming on roots of plants grown in Transparent soil
777 (Downie et al., 2012). (b) *Heterodera schachtii* feeding on roots infected with Tobacco rattle
778 virus expressing mRFP protein to visualise the uptake of mRFP by the nematode during
779 feeding (unpublished image - Valentine et al. (2007)). X-ray CT utilised to image Setona
780 seeking out root nodules in an intact root:soil sample (Johnson et al., 2004). (d) Physical
781 interactions: Neutron radiography image of roots (left) with image of oxygen gradients (right)
782 obtained using oxygen sensitive foil (Rudolph et al., 2012). (e) Analysis of root soil contact,
783 blue represents areas of root surface in contact with soil particles (Schmidt et al., 2012). (f)
784 Dynamic root growth analysis using PIV showing movement of surrounding constraining
785 growth medium in response to root penetration (Bengough et al., 2010). (g) Synchrotron data
786 enabling visualisation of root hair contact in intact soil samples (Keyes et al., 2013). (h)
787 Fluorescence based (CLSM) imaging to visualise root hair particle interactions in transparent
788 soil (Previously unpublished image - (Downie et al., 2012). (a), Reproduced under Creative
789 Commons Attribution License. (b) Previously unpublished image. (c, e, f, g) Reproduced
790 with kind permission from John Wiley & Sons. (d) Reproduced with kind permission from
791 Springer Science and Business media.

792

793 **Figure 5. Decision process for root phenotyping pipeline**

794 Phenotyping the rhizosphere via image analysis requires several inter connecting steps, each
795 with many parameters that need to be considered. Each parameter may impact on the
796 downstream processing of the images or may alter the number of images and the type of
797 images that it is necessary to acquired earlier in the analysis pipeline

798

799

800 **REFERENCES**

- 801 Abbas-Zadeh P., Saleh-Rastin N., Asadi-Rahmani H., Khavazi K., Soltani A., Shoary-Nejati A.R.
802 & Miransari M. (2010) Plant growth-promoting activities of fluorescent
803 pseudomonads, isolated from the Iranian soils. *Acta Physiologiae Plantarum*, **32**,
804 281-288.
- 805 Adu M.O., Wiesel L., Bennett M.J., Broadley M.R., White P.J. & Dupuy L.X. (2014) A scanner
806 system for high-resolution quantification of variation in root growth dynamics of
807 Brassica rapa genotypes. *Journal of Experimental Botany*, **65**, 2039-2048.
- 808 al Hagrey S.A. (2007) Geophysical imaging of root-zone, trunk, and moisture heterogeneity.
809 *Journal of Experimental Botany*, **58**, 839-854.
- 810 Amato M., Bitella G., Rossi R., Gomez J.A., Lovelli S. & Ferreira Gomes J.J. (2009) Multi-
811 electrode 3D resistivity imaging of alfalfa root zone. *European Journal of Agronomy*,
812 **31**, 213-222.
- 813 Amos B.R., E.; Reichelt, S.; (2010) Improving the magnifying glass: a new giant lens.
- 814 Armengaud P., Zambaux K., Hills A., Sulpice R., Pattison R.J., Blatt M.R. & Amtmann A. (2009)
815 EZ-Rhizo: integrated software for the fast and accurate measurement of root system
816 architecture. *Plant Journal*, **57**, 945-956.
- 817 Asseng S., Keating B.A., Fillery I.R.P., Gregory P.J., Bowden J.W., Turner N.C., . . . ,Abrecht D.G.
818 (1998) Performance of the APSIM-wheat model in Western Australia. *Field Crops*
819 *Research*, **57**, 163-179.
- 820 Bailey D.J., Kleczkowski A. & Gilligan C.A. (2006) An epidemiological analysis of the role of
821 disease-induced root growth in the differential response of two cultivars of winter
822 wheat to infection by Gaeumannomyces graminis var. tritici. *Phytopathology*, **96**,
823 510-516.
- 824 Balasubramanian S., Schwartz C., Singh A., Warthmann N., Kim M.C., Maloof J.N., . . . ,Weigel
825 D. (2009) QTL Mapping in New Arabidopsis thaliana Advanced Intercross-
826 Recombinant Inbred Lines. *Plos One*, **4**, e4318.
- 827 Baldwin J.P., Tinker P.B. & Marriott F.H. (1971) Measurement of length and distribution of
828 onion roots in field and laboratory. *Journal of Applied Ecology*, **8**, 543-554.
- 829 Bao Y., Aggarwal P., Robbins N.E., 2nd, Sturrock C.J., Thompson M.C., Tan H.Q., . . . ,Dinneny
830 J.R. (2014) Plant roots use a patterning mechanism to position lateral root branches
831 toward available water. *Proceedings of the National Academy of Sciences of the*
832 *United States of America*, **111**, 9319-9324.
- 833 Barton C.V.M. & Montagu K.D. (2004) Detection of tree roots and determination of root
834 diameters by ground penetrating radar under optimal conditions. *Tree Physiology*,
835 **24**, 1323-1331.
- 836 Basu P. & Pal A. (2012) A new tool for analysis of root growth in the spatio-temporal
837 continuum. *New Phytologist*, **195**, 264-274.
- 838 Bates G.H. (1937) A Device for the Observation of Root Growth in the Soil. *Nature Methods*,
839 **139**, 966-967.
- 840 Batey T. (2009) Soil compaction and soil management - a review. *Soil Use and Management*,
841 **25**, 335-345.
- 842 Bauer W.D. & Mathesius U. (2004) Plant responses to bacterial quorum sensing signals.
843 *Current Opinion in Plant Biology*, **7**, 429-433.
- 844 Beemster G.T.S. & Baskin T.I. (1998) Analysis of cell division and elongation underlying the
845 developmental acceleration of root growth in Arabidopsis thaliana. *Plant Physiology*,
846 **116**, 1515-1526.

847 Bengough A.G., Gordon D.C., Al-Menaie H., Ellis R.P., Allan D., Keith R., . . . ,Forster B.P. (2004)
848 Gel observation chamber for rapid screening of root traits in cereal seedlings. *Plant*
849 *and Soil*, **262**, 63-70.

850 Bengough A.G., Hans J., Bransby M.F. & Valentine T.A. (2010) PIV as a Method for
851 Quantifying Root Cell Growth and Particle Displacement in Confocal Images.
852 *Microscopy Research and Technique*, **73**, 27-36.

853 Bengough A.G., McKenzie B.M., Hallett P.D. & Valentine T.A. (2011) Root elongation, water
854 stress, and mechanical impedance: a review of limiting stresses and beneficial root
855 tip traits. *Journal of Experimental Botany*, **62**, 59-68.

856 Benjamin J.G. & Nielsen D.C. (2004) A method to separate plant roots from soil and analyze
857 root surface area. *Plant and Soil*, **267**, 225-234.

858 Berendsen R.L., Pieterse C.M.J. & Bakker P.A.H.M. (2012) The rhizosphere microbiome and
859 plant health. *Trends in Plant Science*, **17**, 478-486.

860 Bingham I.J. & Bengough A.G. (2003) Morphological plasticity of wheat and barley roots in
861 response to spatial variation in soil strength. *Plant and Soil*, **250**, 273-282.

862 Bloemberg G.V., Wijfjes A.H.M., Lamers G.E.M., Stuurman N. & Lugtenberg B.J.J. (2000)
863 Simultaneous imaging of *Pseudomonas fluorescens* WCS365 populations expressing
864 three different autofluorescent proteins in the rhizosphere: New perspectives for
865 studying microbial communities. *Molecular Plant-Microbe Interactions*, **13**, 1170-
866 1176.

867 Blossfeld S. & Gansert D. (2007) A novel non-invasive optical method for quantitative
868 visualization of pH dynamics in the rhizosphere of plants. *Plant Cell and Environment*,
869 **30**, 176-186.

870 Blossfeld S., Gansert D., Thiele B., Kuhn A.J. & Loesch R. (2011) The dynamics of oxygen
871 concentration, pH value, and organic acids in the rhizosphere of *Juncus* spp. *Soil*
872 *Biology & Biochemistry*, **43**, 1186-1197.

873 Blossfeld S., Perriguet J., Sterckeman T., Morel J.-L. & Loesch R. (2010) Rhizosphere pH
874 dynamics in trace-metal-contaminated soils, monitored with planar pH optodes.
875 *Plant and Soil*, **330**, 173-184.

876 Blossfeld S., Schreiber C.M., Liebsch G., Kuhn A.J. & Hinsinger P. (2013) Quantitative imaging
877 of rhizosphere pH and CO₂ dynamics with planar optodes. *Annals of Botany*, **112**,
878 267-276.

879 Bohn W. (1979) *Methods of Studying Root Systems*. Springer-Verlag, Berlin.

880 Bois J.F. & Couchat P. (1983) Comparison of the effects of water-stress on the root systems of
881 2 cultivars of upland rice (*Oryza-sativa*-L). *Annals of Botany*, **52**, 479-487.

882 Bottomley P.A., Rogers H.H. & Foster T.H. (1986) NMR imaging shows water distribution and
883 transport in plant-root systems *insitu*. *Proceedings of the National Academy of*
884 *Sciences of the United States of America*, **83**, 87-89.

885 Bougourd S., Marrison J. & Haseloff J. (2000) An aniline blue staining procedure for confocal
886 microscopy and 3D imaging of normal and perturbed cellular phenotypes in mature
887 *Arabidopsis* embryos. *Plant Journal*, **24**, 543-550.

888 Bovina R., Brunazzi A., Gasparini G., Sestili F., Palombieri S., Botticella E., . . . ,Massi A. (2014)
889 Development of a TILLING resource in durum wheat for reverse- and forward-
890 genetic analyses. *Crop & Pasture Science*, **65**, 112-124.

891 Brady S.M., Orlando D.A., Lee J.-Y., Wang J.Y., Koch J., Dinneny J.R., . . . ,Benfey P.N. (2007) A
892 high-resolution root spatiotemporal map reveals dominant expression patterns.
893 *Science*, **318**, 801-806.

894 Brooks T.L.D., Miller N.D. & Spalding E.P. (2010) Plasticity of Arabidopsis Root Gravitropism
895 throughout a Multidimensional Condition Space Quantified by Automated Image
896 Analysis. *Plant Physiology*, **152**, 206-216.

897 Brown L.K., George T.S., Thompson J.A., Wright G., Lyon J., Dupuy L., . . . , White P.J. (2012)
898 What are the implications of variation in root hair length on tolerance to phosphorus
899 deficiency in combination with water stress in barley (*Hordeum vulgare*)? *Annals of*
900 *Botany*, **110**, 319-328.

901 Bruand A., Cousin I., Nicoullaud B., Duval O. & Begon J.C. (1996) Backscattered electron
902 scanning images of soil porosity for analyzing soil compaction around roots. *Soil*
903 *Science Society of America Journal*, **60**, 895-901.

904 Burton A.L., Lynch J.P. & Brown K.M. (2013) Spatial distribution and phenotypic variation in
905 root cortical aerenchyma of maize (*Zea mays* L.). *Plant and Soil*, **367**, 263-274.

906 Burton A.L., Williams M., Lynch J.P. & Brown K.M. (2012) RootScan: Software for high-
907 throughput analysis of root anatomical traits. *Plant and Soil*, **357**, 189-203.

908 Caldwell D.G., McCallum N., Shaw P., Muehlbauer G.J., Marshall D.F. & Waugh R. (2004) A
909 structured mutant population for forward and reverse genetics in Barley (*Hordeum*
910 *vulgare* L.). *Plant Journal*, **40**, 143-150.

911 Carminati A. & Fluehler H. (2009) Water Infiltration and Redistribution in Soil Aggregate
912 Packings. *Vadose Zone Journal*, **8**, 150-157.

913 Carminati A., Moradi A.B., Vetterlein D., Vontobel P., Lehmann E., Weller U., . . . , Oswald S.E.
914 (2010) Dynamics of soil water content in the rhizosphere. *Plant and Soil*, **332**, 163-
915 176.

916 Chaparro J.M., Sheflin A.M., Manter D.K. & Vivanco J.M. (2012) Manipulating the soil
917 microbiome to increase soil health and plant fertility. *Biology and Fertility of Soils*, **48**,
918 489-499.

919 Chapman S., Oparka K.J. & Roberts A.G. (2005) New tools for in vivo fluorescence tagging.
920 *Current Opinion in Plant Biology*, **8**, 565-573.

921 Clark E.L., Daniell T.J., Wishart J., Hubbard S.F. & Karley A.J. (2012) How Conserved Are the
922 Bacterial Communities Associated With Aphids? A Detailed Assessment of the
923 *Brevicoryne brassicae* (Hemiptera: Aphididae) Using 16S rDNA. *Environmental*
924 *Entomology*, **41**, 1386-1397.

925 Clark L.J., Whalley W.R., Leigh R.A., Dexter A.R. & Barraclough P.B. (1999) Evaluation of agar
926 and agarose gels for studying mechanical impedance in rice roots. *Plant and Soil*, **207**,
927 37-43.

928 Clark R.T., Famoso A.N., Zhao K., Shaff J.E., Craft E.J., Bustamante C.D., . . . , Kochian L.V.
929 (2013) High-throughput two-dimensional root system phenotyping platform
930 facilitates genetic analysis of root growth and development. *Plant Cell and*
931 *Environment*, **36**, 454-466.

932 Clark R.T., MacCurdy R.B., Jung J.K., Shaff J.E., McCouch S.R., Aneshansley D.J. & Kochian L.V.
933 (2011) Three-Dimensional Root Phenotyping with a Novel Imaging and Software
934 Platform. *Plant Physiology*, **156**, 455-465.

935 Czarnes S., Hallett P.D., Bengough A.G. & Young I.M. (2000) Root- and microbial-derived
936 mucilages affect soil structure and water transport. *European Journal of Soil Science*,
937 **51**, 435-443.

938 Czymmek K.J., Fogg M., Powell D.H., Sweigard J., Park S.-Y. & Kang S. (2007) In vivo time-
939 lapse documentation using confocal and multi-photon microscopy reveals the
940 mechanisms of invasion into the Arabidopsis root vascular system by *Fusarium*
941 *oxysporum*. *Fungal Genetics and Biology*, **44**, 1011-1023.

942 Dai X., Wang Y., Yang A. & Zhang W.-H. (2012) OsMYB2P-1, an R2R3 MYB Transcription
943 Factor, Is Involved in the Regulation of Phosphate-Starvation Responses and Root
944 Architecture in Rice. *Plant Physiology*, **159**, 169-183.

945 Dannoura M., Kominami Y., Makita N. & Oguma H. (2012) Flat Optical Scanner Method and
946 Root Dynamics. In: *Measuring Roots: An Updated Approach* (ed S. Mancuso), pp.
947 127-133.

948 Darwin C. (1880) *The power of movement in plants*. John Murray, London.

949 Dechamps C., Noret N., Mozek R., Draye X. & Meerts P. (2008) Root allocation in metal-rich
950 patch by *Thlaspi caerulescens* from normal and metalliferous soil - new insights into
951 the rhizobox approach. *Plant and Soil*, **310**, 211-224.

952 Delhaize E., James R.A. & Ryan P.R. (2012) Aluminium tolerance of root hairs underlies
953 genotypic differences in rhizosheath size of wheat (*Triticum aestivum*) grown on acid
954 soil. *New Phytologist*, **195**, 609-619.

955 Delin S. & Stromberg N. (2011) Imaging-optode measurements of ammonium distribution in
956 soil after different manure amendments. *European Journal of Soil Science*, **62**, 295-
957 304.

958 Den Herder G., Van Isterdael G., Beeckman T. & De Smet I. (2010) The roots of a new green
959 revolution. *Trends in Plant Science*, **15**, 600-607.

960 Dhondt S., Wuyts N. & Inze D. (2013) Cell to whole-plant phenotyping: the best is yet to
961 come. *Trends in Plant Science*, **18**, 433-444.

962 Dietrich R.C., Bengough A.G., Jones H.G. & White P.J. (2013) Can root electrical capacitance
963 be used to predict root mass in soil? *Annals of botany*, **112**, 457-464.

964 Dixit R., Cyr R. & Gilroy S. (2006) Using intrinsically fluorescent proteins for plant cell imaging.
965 *Plant Journal*, **45**, 599-615.

966 Dong S.F., Neilsen D., Neilsen G.H. & Weis M. (2003) A scanner-based root image acquisition
967 technique for measuring roots on a rhizotron window. *Hortscience*, **38**, 1385-1388.

968 Donner E., Punshon T., Guerinot M.L. & Lombi E. (2012) Functional characterisation of
969 metal(loid) processes in planta through the integration of synchrotron techniques
970 and plant molecular biology. *Analytical and Bioanalytical Chemistry*, **402**, 3287-3298.

971 Downie H., Holden N., Otten W., Spiers A.J., Valentine T.A. & Dupuy L.X. (2012) Transparent
972 Soil for Imaging the Rhizosphere. *Plos One*, **7**, e44276.

973 Downie H.F., Valentine T.A., Otten W., Spiers A.J. & Dupuy L.X. (2014) Transparent soil
974 microcosms allow 3D spatial quantification of soil microbiological processes in vivo.
975 *Plant Signaling & Behavior*, **9**, e29878.

976 Draye X., Kim Y., Lobet G. & Javaux M. (2010) Model-assisted integration of physiological and
977 environmental constraints affecting the dynamic and spatial patterns of root water
978 uptake from soils. *Journal of Experimental Botany*, **61**, 2145-2155.

979 Dubrovsky J.G. & Forde B.G. (2012) Quantitative Analysis of Lateral Root Development:
980 Pitfalls and How to Avoid Them. *Plant Cell*, **24**, 4-14.

981 Duncan J.S. & Ayache N. (2000) Medical image analysis: Progress over two decades and the
982 challenges ahead. *Ieee Transactions on Pattern Analysis and Machine Intelligence*, **22**,
983 85-106.

984 Ehlers W., Kopke U., Hesse F. & Bohm W. (1983) Penetration resistance and root-growth of
985 oats in tilled and untilled loess soil. *Soil & Tillage Research*, **3**, 261-275.

986 Eickhorst T. & Tippkoetter R. (2008) Improved detection of soil microorganisms using
987 fluorescence in situ hybridization (FISH) and catalyzed reporter deposition (CARD-
988 FISH). *Soil Biology & Biochemistry*, **40**, 1883-1891.

- 989 Faget M., Blossfeld S., von Gillhaussen P., Schurr U. & Temperton V.M. (2013) Disentangling
 990 who is who during rhizosphere acidification in root interactions: combining
 991 fluorescence with optode techniques. *Frontiers in Plant Science*, **4**, 392.
- 992 Faget M., Herrera J.M., Stamp P., Aulinger-Leipner I., Frossard E. & Liedgens M. (2009) The
 993 use of green fluorescent protein as a tool to identify roots in mixed plant stands.
 994 *Functional Plant Biology*, **36**, 930-937.
- 995 Faget M.N., K.A.; Walter, A.; Herrera, J.M.; Jahnke, S.; Schurr, U.; Temperton, V.M. (2013)
 996 Root-root interactions: extending our perspective to be more inclusive of the range
 997 of theories in ecology and agriculture using in-vivo analyses. *Annals of Botany*, **112**,
 998 253-266.
- 999 Fang S., Gao X., Deng Y., Chen X. & Liao H. (2011) Crop Root Behavior Coordinates
 1000 Phosphorus Status and Neighbors: From Field Studies to Three-Dimensional in Situ
 1001 Reconstruction of Root System Architecture. *Plant Physiology*, **155**, 1277-1285.
- 1002 Fang S., Yan X. & Liao H. (2009) 3D reconstruction and dynamic modeling of root
 1003 architecture in situ and its application to crop phosphorus research. *Plant Journal*,
 1004 **60**, 1096-1108.
- 1005 Federici F., Dupuy L., Laplace L., Heisler M. & Haseloff J. (2012) Integrated genetic and
 1006 computation methods for in planta cytometry. *Nature Methods*, **9**, 483-U104.
- 1007 Fiorani F. & Schurr U. (2013) Future Scenarios for Plant Phenotyping. In: *Annual Review of*
 1008 *Plant Biology*, Vol 64 (ed S.S. Merchant), pp. 267-291.
- 1009 Fisher M.E., Clelland A.K., Bain A., Baldock R.A., Murphy P., Downie H., . . . , Buckland R.A.
 1010 (2008) Integrating technologies for comparing 3D gene expression domains in the
 1011 developing chick limb. *Developmental Biology*, **317**, 13-23.
- 1012 Frangi A.F., Niessen W.J., Vincken K.L. & Viergever M.A. (1998) Multiscale vessel
 1013 enhancement filtering. In: *Medical Image Computing and Computer-Assisted*
 1014 *Intervention - Miccai'98* (eds W.M. Wells, A. Colchester, & S. Delp), pp. 130-137.
- 1015 French A., Ubeda-Tomas S., Holman T.J., Bennett M.J. & Pridmore T. (2009) High-Throughput
 1016 Quantification of Root Growth Using a Novel Image-Analysis Tool. *Plant Physiology*,
 1017 **150**, 1784-1795.
- 1018 French A., Wells D., Everitt N. & Pridmore T. (2012) High-Throughput Quantification of Root
 1019 Growth. In: *Measuring Roots: An Updated Approach* (ed S. Mancuso), pp. 109-126.
- 1020 Gage D.J., Bobo T. & Long S.R. (1996) Use of green fluorescent protein to visualize the early
 1021 events of symbiosis between *Rhizobium meliloti* and alfalfa (*Medicago sativa*).
 1022 *Journal of Bacteriology*, **178**, 7159-7166.
- 1023 Galkovskiy T., Mileyko Y., Bucksch A., Moore B., Symonova O., Price C.A., . . . , Weitz J.S.
 1024 (2012) GiA Roots: software for the high throughput analysis of plant root system
 1025 architecture. *Bmc Plant Biology*, **12**, 116.
- 1026 Gamalero E., Lingua G., Tombolini R., Avidano L., Pivato B. & Berta G. (2005) Colonization of
 1027 tomato root seedling by *Pseudomonas fluorescens* 92rkG5: Spatio-temporal
 1028 dynamics, localization, organization, viability, and culturability. *Microbial Ecology*, **50**,
 1029 289-297.
- 1030 Garbout A., Munkholm L.J., Hansen S.B., Petersen B.M., Munk O.L. & Pajor R. (2012) The use
 1031 of PET/CT scanning technique for 3D visualization and quantification of real-time
 1032 soil/plant interactions. *Plant and Soil*, **352**, 113-127.
- 1033 Gasch C.K., Collier T.R., Enloe S.F. & Prager S.D. (2011) A GIS-based method for the analysis
 1034 of digital rhizotron images. *Plant Root*, **5**, 69-78.
- 1035 Genre A. & Bonfante P. (2005) Building a mycorrhizal cell: How to reach compatibility
 1036 between plants and arbuscular mycorrhizal fungi. *Journal of Plant Interactions*, **1**, 3-
 1037 13.

- 1038 George T.S., Brown L.K., Ramsay L., White P.J., Newton A.C., Bengough A.G., . . . ,Thomas
1039 W.T.B. (2014) Understanding the genetic control and physiological traits associated
1040 with rhizosheath production by barley (*Hordeum vulgare*). *New Phytologist*, **203**,
1041 195-205.
- 1042 Goh C.-H., Vallejos D.F.V., Nicotra A.B. & Mathesius U. (2013) The Impact of Beneficial Plant-
1043 Associated Microbes on Plant Phenotypic Plasticity. *Journal of Chemical Ecology*, **39**,
1044 826-839.
- 1045 Gomiero T., Pimentel D. & Paoletti M.G. (2011) Is There a Need for a More Sustainable
1046 Agriculture? *Critical Reviews in Plant Sciences*, **30**, 6-23.
- 1047 Gregory P.J., Bengough A.G., Grinev D., Schmidt S., Thomas W.T.B., Wojciechowski T. &
1048 Young I.M. (2009a) Root phenomics of crops: opportunities and challenges.
1049 *Functional Plant Biology*, **36**, 922-929.
- 1050 Gregory P.J., Hutchison D.J., Read D.B., Jenneson P.M., Gilboy W.B. & Morton E.J. (2003)
1051 Non-invasive imaging of roots with high resolution X-ray micro-tomography. *Plant
1052 and Soil*, **255**, 351-359.
- 1053 Gregory P.J., Johnson S.N., Newton A.C. & Ingram J.S.I. (2009b) Integrating pests and
1054 pathogens into the climate change/food security debate. *Journal of Experimental
1055 Botany*, **60**, 2827-2838.
- 1056 Grose M.J., Gilligan C.A., Spencer D. & Goddard B.V.D. (1996) Spatial heterogeneity of soil
1057 water around single roots: Use of CT-scanning to predict fungal growth in the
1058 rhizosphere. *New Phytologist*, **133**, 261-272.
- 1059 Grzesiak S., Grzesiak M.T., Felek W., Hura T. & Stabryla J. (2002) The impact of different soil
1060 moisture and soil compaction on the growth of triticale root system. *Acta
1061 Physiologiae Plantarum*, **24**, 331-342.
- 1062 Hainsworth J.M. & Aylmore L.A.G. (1983) The use of computer-assisted tomography to
1063 determine spatial-distribution of soil-water content. *Australian Journal of Soil
1064 Research*, **21**, 435-443.
- 1065 Haling R.E., Brown L.K., Bengough A.G., Valentine T.A., White P.J., Young I.M. & George T.S.
1066 (2014) Root hair length and rhizosheath mass depend on soil porosity, strength and
1067 water content in barley genotypes. *Planta*, **239**, 643-651.
- 1068 Hammond J.P. & White P.J. (2008) Sucrose transport in the phloem: integrating root
1069 responses to phosphorus starvation. *Journal of Experimental Botany*, **59**, 93-109.
- 1070 Hamza M.A., Anderson S.H. & Aylmore L.A.G. (2001) Studies of soil water drawdowns by
1071 single radish roots at decreasing soil water content using computer-assisted
1072 tomography. *Australian Journal of Soil Research*, **39**, 1387-1396.
- 1073 Hamza M.A. & Aylmore L.A.G. (1992) Soil solute concentration and water-uptake by single
1074 lupin and radish plant-roots .1. Water extraction and solute accumulation. *Plant and
1075 Soil*, **145**, 187-196.
- 1076 Harris K., Crabb D., Young I.M., Weaver H., Gilligan C.A., Otten W. & Ritz K. (2002) In situ
1077 visualisation of fungi in soil thin sections: problems with crystallisation of the
1078 fluorochrome FB 28 (Calcofluor M2R) and improved staining by SCRI Renaissance
1079 2200. *Mycological Research*, **106**, 293-297.
- 1080 Haynes J.G., Czymmek K.J., Carlson C.A., Veereshlingam H., Dickstein R. & Sherrier D.J. (2004)
1081 Rapid analysis of legume root nodule development using confocal microscopy. *New
1082 Phytologist*, **163**, 661-668.
- 1083 Heeraman D.A., Hopmans J.W. & Clausnitzer V. (1997) Three dimensional imaging of plant
1084 roots in situ with x-ray computed tomography. *Plant and Soil*, **189**, 167-179.

- 1085 Herrera J.M.V., N.; Govaerts, B. (2012) Strategies to identify genetic diversity in root traits. In:
 1086 *Physiological breeding I: interdisciplinary approaches to improve crop adaptation* (ed
 1087 M.P.P.A.J.D.M. Reynolds, D.), pp. 97-108. CIMMYT, Mexico, DF.
- 1088 Hiltner L. (1904) Über neue Erfahrungen und Probleme auf dem Gebiete der
 1089 Bodenbakteriologie. *Arbeiten der Deutschen Landwirtschaftsgesellschaft*, **98**, 19.
- 1090 Hu B., Henry A., Brown K.M. & Lynch J.P. (2014) Root cortical aerenchyma inhibits radial
 1091 nutrient transport in maize (*Zea mays*). *Annals of Botany*, **113**, 181-189.
- 1092 Huisken J., Swoger J., Del Bene F., Wittbrodt J. & Stelzer E.H.K. (2004) Optical sectioning
 1093 deep inside live embryos by selective plane illumination microscopy. *Science*, **305**,
 1094 1007-1009.
- 1095 Humphris S.N., Bengough A.G., Griffiths B.S., Kilham K., Rodger S., Stubbs V., . . . ,Young I.M.
 1096 (2005) Root cap influences root colonisation by *Pseudomonas fluorescens* SBW25 on
 1097 maize. *Fems Microbiology Ecology*, **54**, 123-130.
- 1098 Hund A., Trachsel S. & Stamp P. (2009) Growth of axile and lateral roots of maize: I
 1099 development of a phenotyping platform. *Plant and Soil*, **325**, 335-349.
- 1100 Ishikawa S., Suzui N., Ito-Tanabata S., Ishii S., Igura M., Abe T., . . . ,Fujimaki S. (2011) Real-
 1101 time imaging and analysis of differences in cadmium dynamics in rice cultivars
 1102 (*Oryza sativa*) using positron-emitting Cd-107 tracer. *Bmc Plant Biology*, **11**, 172.
- 1103 Jahnke S., Menzel M.I., van Dusschoten D., Roeb G.W., Buhler J., Minwuyet S., . . . ,Schurr
 1104 U. (2009) Combined MRI-PET dissects dynamic changes in plant structures and
 1105 functions. *Plant Journal*, **59**, 634-644.
- 1106 Jassogne L., Hettiarachchi G., Chittleborough D. & McNeill A. (2009) Distribution and
 1107 Speciation of Nutrient Elements around Micropores. *Soil Science Society of America
 1108 Journal*, **73**, 1319-1326.
- 1109 Johnson S.N., Read D.B. & Gregory P.J. (2004) Tracking larval insect movement within soil
 1110 using high resolution X-ray microtomography. *Ecological Entomology*, **29**, 117-122.
- 1111 Kaestner A., Schneebeli M. & Graf F. (2006) Visualizing three-dimensional root networks
 1112 using computed tomography. *Geoderma*, **136**, 459-469.
- 1113 Kell D.B. (2011) Breeding crop plants with deep roots: their role in sustainable carbon,
 1114 nutrient and water sequestration. *Annals of Botany*, **108**, 407-418.
- 1115 Ketcham R.A. & Carlson W.D. (2001) Acquisition, optimization and interpretation of X-ray
 1116 computed tomographic imagery: applications to the geosciences. *Computers &
 1117 Geosciences*, **27**, 381-400.
- 1118 Keyes S.D., Daly K.R., Gostling N.J., Jones D.L., Talboys P., Pinzer B.R., . . . ,Roose T. (2013)
 1119 High resolution synchrotron imaging of wheat root hairs growing in soil and image
 1120 based modelling of phosphate uptake. *New Phytologist*, **198**, 1023-1029.
- 1121 King F.H. (1883) The influence of gravitation, moisture, and light upon the direction of
 1122 growth in the root and stem of plants. *Science*, **2**, 5-6.
- 1123 Kiser M.R., Reid C.D., Crowell A.S., Phillips R.P. & Howell C.R. (2008) Exploring the transport
 1124 of plant metabolites using positron emitting radiotracers. *Hfsp Journal*, **2**, 189-204.
- 1125 Kreike C.M., KokWesteneng A.A., Vinke J.H. & Stiekema W.J. (1996) Mapping of QTLs
 1126 involved in nematode resistance, tuber yield and root development in *Solanum* sp.
 1127 *Theoretical and Applied Genetics*, **92**, 463-470.
- 1128 Kuchenbuch R.O. & Ingram K.T. (2002) Image analysis for non-destructive and non-invasive
 1129 quantification of root growth and soil water content in rhizotrons. *Journal of Plant
 1130 Nutrition and Soil Science-Zeitschrift Fur Pflanzenernahrung Und Bodenkunde*, **165**,
 1131 573-581.
- 1132 Kutschera L. (1960) *Wurzelatlas mitteleuropäischer Ackerunkräuter und Kulturpflanzen*. DLG
 1133 Verlag, Frankfurt-am-Main.

1134 Lambers H., Mougel C., Jaillard B. & Hinsinger P. (2009) Plant-microbe-soil interactions in the
1135 rhizosphere: an evolutionary perspective. *Plant and Soil*, **321**, 83-115.

1136 Lebreton C., Lazicjancic V., Steed A., Pekic S. & Quarrie S.A. (1995) Identification of QTL for
1137 drought responses in maize and their use in testing causal relationships between
1138 traits. *Journal of Experimental Botany*, **46**, 853-865.

1139 Lee K., Avondo J., Morrison H., Blot L., Stark M., Sharpe J., . . . , Coen E. (2006) Visualizing
1140 plant development and gene expression in three dimensions using optical projection
1141 tomography. *Plant Cell*, **18**, 2145-2156.

1142 Lind K.R., Sizmur T., Benomar S., Miller A. & Cademartiri L. (2014) LEGO Bricks as Building
1143 Blocks for Centimeter-Scale Biological Environments: The Case of Plants. *PloS one*, **9**,
1144 e100867.

1145 Lobet G., Draye X. & Perilleux C. (2013) An online database for plant image analysis software
1146 tools. *Plant Methods*, **9**, 38.

1147 Lobet G., Pagès L. & Draye X. (2011) A novel image-analysis toolbox enabling quantitative
1148 analysis of root system architecture. *Plant physiology*, **157**, 29-39.

1149 Lontoc-Roy M., Dutilleul P., Prasher S.O., Han L., Brouillet T. & Smith D.L. (2006) Advances in
1150 the acquisition and analysis of CT scan data to isolate a crop root system from the
1151 soil medium and quantify root system complexity in 3-D space. *Geoderma*, **137**, 231-
1152 241.

1153 Lopez-Bucio J., Hernandez-Abreu E., Sanchez-Calderon L., Nieto-Jacobo M.F., Simpson J. &
1154 Herrera-Estrella L. (2002) Phosphate availability alters architecture and causes
1155 changes in hormone sensitivity in the Arabidopsis root system. *Plant Physiology*, **129**,
1156 244-256.

1157 Loudet O., Chaillou S., Camilleri C., Bouchez D. & Daniel-Vedele F. (2002) Bay-0 x Shahdara
1158 recombinant inbred line population: a powerful tool for the genetic dissection of
1159 complex traits in Arabidopsis. *Theoretical and Applied Genetics*, **104**, 1173-1184.

1160 Luster J., Goettlein A., Nowack B. & Sarret G. (2009) Sampling, defining, characterising and
1161 modeling the rhizosphere-the soil science tool box. *Plant and Soil*, **321**, 457-482.

1162 Lynch J.P. (2013) Steep, cheap and deep: an ideotype to optimize water and N acquisition by
1163 maize root systems. *Annals of Botany*, **112**, 347-357.

1164 Macfall J.S., Johnson G.A. & Kramer P.J. (1990) Observation of a water-depletion region
1165 surrounding Loblolly-pine roots by magnetic-resonance-imaging. *Proceedings of the
1166 National Academy of Sciences of the United States of America*, **87**, 1203-1207.

1167 Macfall J.S., Johnson G.A. & Kramer P.J. (1991) Comparative water-uptake by roots of
1168 different ages in seedlings of Loblolly-pine (*Pinus-taeda* L). *New Phytologist*, **119**,
1169 551-560.

1170 Mairhofer S., Zappala S., Tracy S.R., Sturrock C., Bennett M., Mooney S.J. & Pridmore T.
1171 (2012) RooTrak: Automated Recovery of Three-Dimensional Plant Root Architecture
1172 in Soil from X-Ray Microcomputed Tomography Images Using Visual Tracking. *Plant
1173 Physiology*, **158**, 561-569.

1174 Maizel A., von Wangenheim D., Federici F., Haseloff J. & Stelzer E.H.K. (2011) High-resolution
1175 live imaging of plant growth in near physiological bright conditions using light sheet
1176 fluorescence microscopy. *Plant Journal*, **68**, 377-385.

1177 Martino E., Murat C., Vallino M., Bena A., Perotto S. & Spanu P. (2007) Imaging mycorrhizal
1178 fungal transformants that express EGFP during ericoid endosymbiosis. *Current
1179 Genetics*, **52**, 65-75.

1180 McKenzie B.M., Bengough A.G., Hallett P.D., Thomas W.T.B., Forster B. & McNicol J.W. (2009)
1181 Deep rooting and drought screening of cereal crops: A novel field-based method and
1182 its application. *Field Crops Research*, **112**, 165-171.

- 1183 Metscher B.D. & Mueller G.B. (2011) MicroCT for Molecular Imaging: Quantitative
 1184 Visualization of Complete Three-Dimensional Distributions of Gene Products in
 1185 Embryonic Limbs. *Developmental Dynamics*, **240**, 2301-2308.
- 1186 Mir R.R., Zaman-Allah M., Sreenivasulu N., Trethowan R. & Varshney R.K. (2012) Integrated
 1187 genomics, physiology and breeding approaches for improving drought tolerance in
 1188 crops. *Theoretical and Applied Genetics*, **125**, 625-645.
- 1189 Mooney S.J., Pridmore T.P., Helliwell J. & Bennett M.J. (2012) Developing X-ray Computed
 1190 Tomography to non-invasively image 3-D root systems architecture in soil. *Plant and
 1191 Soil*, **352**, 1-22.
- 1192 Moradi A.B., Carminati A., Vetterlein D., Vontobel P., Lehmann E., Weller U., . . . ,Oswald S.E.
 1193 (2011) Three-dimensional visualization and quantification of water content in the
 1194 rhizosphere. *New Phytologist*, **192**, 653-663.
- 1195 Moradi A.B., Conesa H.M., Robinson B., Lehmann E., Kuehne G., Kaestner A., . . . ,Schulin R.
 1196 (2009) Neutron radiography as a tool for revealing root development in soil:
 1197 capabilities and limitations. *Plant and Soil*, **318**, 243-255.
- 1198 Moter A. & Gobel U.B. (2000) Fluorescence in situ hybridization (FISH) for direct visualization
 1199 of microorganisms. *Journal of Microbiological Methods*, **41**, 85-112.
- 1200 Mullen J.L., Wolverton C., Ishikawa H. & Evans M.L. (2000) Kinetics of constant gravitropic
 1201 stimulus responses in Arabidopsis roots using a feedback system. *Plant Physiology*,
 1202 **123**, 665-670.
- 1203 Nagel K.A., Putz A., Gilmer F., Heinz K., Fischbach A., Pfeifer J., . . . ,Schurr U. (2012)
 1204 GROWSCREEN-Rhizo is a novel phenotyping robot enabling simultaneous
 1205 measurements of root and shoot growth for plants grown in soil-filled rhizotrons.
 1206 *Functional Plant Biology*, **39**, 891-904.
- 1207 Neumann G., George T.S. & Plassard C. (2009) Strategies and methods for studying the
 1208 rhizosphere-the plant science toolbox. *Plant and Soil*, **321**, 431-456.
- 1209 Nonomura T., Tajima H., Kitagawa Y., Sekiya N., Shitomi K., Tanaka M., . . . ,Toyoda H. (2003)
 1210 Distinguishable staining with neutral red for GFP-marked and GFP-nonmarked
 1211 *Fusarium oxysporum* strains simultaneously colonizing root surfaces. *Journal of
 1212 General Plant Pathology*, **69**, 45-48.
- 1213 Okumoto S., Jones A. & Frommer W.B. (2012) Quantitative Imaging with Fluorescent
 1214 Biosensors. *Annual Review of Plant Biology*, Vol 63, **63**, 663-706.
- 1215 Ortiz-Ribbing L.M. & Eastburn D.M. (2003) Evaluation of digital image acquisition methods
 1216 for determining soybean root characteristics. *Crop Management*, 1-9.
- 1217 Osmont K.S., Sibout R. & Hardtke C.S. (2007) Hidden branches: Developments in root system
 1218 architecture. In: *Annual Review of Plant Biology*, pp. 93-113.
- 1219 Oswald S.E., Menon M., Carminati A., Vontobel P., Lehmann E. & Schulin R. (2008)
 1220 Quantitative imaging of infiltration, root growth, and root water uptake via neutron
 1221 radiography. *Vadose Zone Journal*, **7**, 1035-1047.
- 1222 Perret J.S., Al-Belushi M.E. & Deadman M. (2007) Non-destructive visualization and
 1223 quantification of roots using computed tomography. *Soil Biology & Biochemistry*, **39**,
 1224 391-399.
- 1225 Pierret A., Capowiez Y., Moran C.J. & Kretschmar A. (1999a) X-ray computed tomography to
 1226 quantify tree rooting spatial distributions. *Geoderma*, **90**, 307-326.
- 1227 Pierret A., Doussan C., Garrigues E. & Mc Kirby J. (2003) Observing plant roots in their
 1228 environment: current imaging options and specific contribution of two-dimensional
 1229 approaches. *Agronomie*, **23**, 471-479.
- 1230 Pierret A., Moran C.J. & Pankhurst C.E. (1999b) Differentiation of soil properties related to
 1231 the spatial association of wheat roots and soil macropores. *Plant and Soil*, **211**, 51-58.

1232 Pohlmeier A., Oros-Peusquens A., Javaux M., Menzel M.I., Vanderborght J., Kaffanke
1233 J., . . . ,Shah N.J. (2008) Changes in soil water content resulting from Ricinus root
1234 uptake monitored by magnetic resonance Imaging. *Vadose Zone Journal*, **7**, 1010-
1235 1017.

1236 Poon K., Hamarneh C. & Abugharbieh R. (2007) Live-vessel: Extending livewire for
1237 simultaneous extraction of optimal medial and boundary paths in vascular images. In:
1238 *Medical Image Computing and Computer-Assisted Intervention- MICCAI 2007, Pt 2,*
1239 *Proceedings* (eds N. Ayache, S. Ourdelin, & A. Maeder), pp. 444-451.

1240 Quarrie S., Lebreton C., Lazic-Jancic V. & Steed A. (1994) QTL for drought responses in an F 2
1241 population. *Maize Genetics Cooperation Newsletter*, 73-74.

1242 Ray J.D., Yu L., McCouch S.R., Champoux M.C., Wang G. & Nguyen H.T. (1996) Mapping
1243 quantitative trait loci associated with root penetration ability in rice (*Oryza sativa* L).
1244 *Theoretical and Applied Genetics*, **92**, 627-636.

1245 Reddy G.V., Gordon S.P. & Meyerowitz E.M. (2007) Unravelling developmental dynamics:
1246 transient intervention and live imaging in plants. *Nature Reviews Molecular Cell*
1247 *Biology*, **8**, 491-501.

1248 Redjala T., Zelko I., Sterckeman T., Legue V. & Lux A. (2011) Relationship between root
1249 structure and root cadmium uptake in maize. *Environmental and Experimental*
1250 *Botany*, **71**, 241-248.

1251 Reynolds M.P., Hellin J., Govaerts B., Kosina P., Sonder K., Hobbs P. & Braun H. (2012) Global
1252 crop improvement networks to bridge technology gaps. *Journal of Experimental*
1253 *Botany*, **63**, 1-12.

1254 Roberts T.J., McKenna S.J., Du C.J., Wuyts N., Valentine T.A. & Bengough A.G. (2010)
1255 Estimating the motion of plant root cells from in vivo confocal laser scanning
1256 microscopy images. *Machine Vision and Applications*, **21**, 921-939.

1257 Rochat L., Pechy-Tarr M., Baehler E., Maurhofer M. & Keel C. (2010) Combination of
1258 Fluorescent Reporters for Simultaneous Monitoring of Root Colonization and
1259 Antifungal Gene Expression by a Biocontrol Pseudomonad on Cereals with Flow
1260 Cytometry. *Molecular Plant-Microbe Interactions*, **23**, 949-961.

1261 Rogers H.H. & Bottomley P.A. (1987) *In situ* nuclear-magnetic-resonance imaging of roots -
1262 influence of soil type, ferromagnetic particle content, and soil-water. *Agronomy*
1263 *Journal*, **79**, 957-965.

1264 Rudolph N., Esser H.G., Carminati A., Moradi A.B., Hilger A., Kardjilov N., . . . ,Oswald S.E.
1265 (2012) Dynamic oxygen mapping in the root zone by fluorescence dye imaging
1266 combined with neutron radiography. *Journal of Soils and Sediments*, **12**, 63-74.

1267 Rudolph N., Voss S., Moradi A.B., Nagl S. & Oswald S.E. (2013) Spatio-temporal mapping of
1268 local soil pH changes induced by roots of lupin and soft-rush. *Plant and Soil*, **369**,
1269 669-680.

1270 Saini A. (2012) MICROSCOPY New Lens Offers Scientist A Brighter Outlook. *Science*, **335**,
1271 1562-1563.

1272 Santi P.A., Johnson S.B., Hillenbrand M., GrandPre P.Z., Glass T.J. & Leger J.R. (2009) Thin-
1273 sheet laser imaging microscopy for optical sectioning of thick tissues. *Biotechniques*,
1274 **46**, 287-294.

1275 Santner J., Zhang H., Leitner D., Schnepf A., Prohaska T., Puschenreiter M. & Wenzel W.W.
1276 (2012) High-resolution chemical imaging of labile phosphorus in the rhizosphere of
1277 *Brassica napus* L. cultivars. *Environmental and Experimental Botany*, **77**, 219-226.

1278 Schmidt S., Bengough A.G., Gregory P.J., Grinev D.V. & Otten W. (2012) Estimating root-soil
1279 contact from 3D X-ray microtomographs. *European Journal of Soil Science*, **63**, 776-
1280 786.

- 1281 Segal E., Kushnir T., Mualem Y. & Shani U. (2008) Microsensing of water dynamics and root
1282 distributions in sandy soils. *Vadose Zone Journal*, **7**, 1018-1026.
- 1283 Sena G., Frentz Z., Birnbaum K.D. & Leibler S. (2011) Quantitation of Cellular Dynamics in
1284 Growing Arabidopsis Roots with Light Sheet Microscopy. *Plos One*, **6**, e21303.
- 1285 Sezgin M. & Sankur B. (2004) Survey over image thresholding techniques and quantitative
1286 performance evaluation. *Journal of Electronic Imaging*, **13**, 146-168.
- 1287 Sharpe J., Ahlgren U., Perry P., Hill B., Ross A., Hecksher-Sorensen J., . . . ,Davidson D. (2002)
1288 Optical projection tomography as a tool for 3D microscopy and gene expression
1289 studies. *Science*, **296**, 541-545.
- 1290 Shi L., Shi T., Broadley M.R., White P.J., Long Y., Meng J., . . . ,Hammond J.P. (2013) High-
1291 throughput root phenotyping screens identify genetic loci associated with root
1292 architectural traits in Brassica napus under contrasting phosphate availabilities.
1293 *Annals of Botany*, **112**, 381-389.
- 1294 Smit A.L.B., A.G.; Engels, C.; Van Noordwijk, M.; Pellerin, S.; Van de Geijn, S.C. (2000) *Root*
1295 *methods: A handbook*. Springer-Verlag New York Inc.; Springer-Verlag GmbH and Co.
1296 KG.
- 1297 Spohn M. & Kuzyakov Y. (2013) Distribution of microbial- and root-derived phosphatase
1298 activities in the rhizosphere depending on P availability and C allocation - Coupling
1299 soil zymography with C-14 imaging. *Soil Biology & Biochemistry*, **67**, 106-113.
- 1300 Stromberg N. (2008) Determination of ammonium turnover and flow patterns close to roots
1301 using Imaging optodes. *Environmental Science & Technology*, **42**, 1630-1637.
- 1302 Tan Z.X., Lal R. & Wiebe K.D. (2005) Global soil nutrient depletion and yield reduction.
1303 *Journal of Sustainable Agriculture*, **26**, 123-146.
- 1304 Thorisson G.A., Muilu J. & Brookes A.J. (2009) Genotype-phenotype databases: challenges
1305 and solutions for the post-genomic era. *Nature Reviews Genetics*, **10**, 9-18.
- 1306 Tilman D., Balzer C., Hill J. & Befort B.L. (2011) Global food demand and the sustainable
1307 intensification of agriculture. *Proceedings of the National Academy of Sciences of the*
1308 *United States of America*, **108**, 20260-20264.
- 1309 Trachsel S., Kaeppler S.M., Brown K.M. & Lynch J.P. (2011) Shovelomics: high throughput
1310 phenotyping of maize (*Zea mays* L.) root architecture in the field. *Plant and Soil*, **341**,
1311 75-87.
- 1312 Tracy S.R., Black C.R., Roberts J.A., McNeill A., Davidson R., Tester M., . . . ,Mooney S.J.
1313 (2012a) Quantifying the effect of soil compaction on three varieties of wheat
1314 (*Triticum aestivum* L.) using X-ray Micro Computed Tomography (CT). *Plant and Soil*,
1315 **353**, 195-208.
- 1316 Tracy S.R., Black C.R., Roberts J.A. & Mooney S.J. (2013) Exploring the interacting effect of
1317 soil texture and bulk density on root system development in tomato (*Solanum*
1318 *lycopersicum* L.). *Environmental and Experimental Botany*, **91**, 38-47.
- 1319 Tracy S.R., Black C.R., Roberts J.A., Sturrock C., Mairhofer S., Craigon J. & Mooney S.J. (2012b)
1320 Quantifying the impact of soil compaction on root system architecture in tomato
1321 (*Solanum lycopersicum*) by X-ray micro-computed tomography. *Annals of Botany*,
1322 **110**, 511-519.
- 1323 Tracy S.R., Roberts J.A., Black C.R., McNeill A., Davidson R. & Mooney S.J. (2010) The X-factor:
1324 visualizing undisturbed root architecture in soils using X-ray computed tomography.
1325 *Journal of Experimental Botany*, **61**, 311-313.
- 1326 Tsaftaris S.A. & Noutsos C. (2009) Plant Phenotyping with Low Cost Digital Cameras and
1327 Image Analytics. In: *Information Technologies in Environmental Engineering* (eds I.N.
1328 Athanasiadis, P.A. Mitkas, A.E. Rizzoli, & J.M. Gomez), pp. 238-251.

1329 Tumlinson L.G., Liu H.Y., Silk W.K. & Hopmans J.W. (2008) Thermal neutron computed
 1330 tomography of soil water and plant roots. *Soil Science Society of America Journal*, **72**,
 1331 1234-1242.
 1332 United Nations D.o.E.a.S.A., Population Division (2013) World Population Prospects: The
 1333 2012 Revision, Key Finding and Advance Table. *ESA/P/WP*, **227**.
 1334 Vacheron J., Desbrosses G., Bouffaud M.-L., Touraine B., Moenne-Loccoz Y., Muller
 1335 D., . . . , Prigent-Combaret C. (2013) Plant growth-promoting rhizobacteria and root
 1336 system functioning. *Frontiers in Plant Science*, **4**, 356.
 1337 Valentine J., Clifton-Brown J., Hastings A., Robson P., Allison G. & Smith P. (2012a) Food vs.
 1338 fuel: the use of land for lignocellulosic next generation' energy crops that minimize
 1339 competition with primary food production. *Global Change Biology Bioenergy*, **4**, 1-19.
 1340 Valentine T., Shaw J., Blok V.C., Phillips M.S., Oparka K.J. & Lacomme C. (2004) Efficient virus-
 1341 induced gene silencing in roots using a modified tobacco rattle virus vector. *Plant*
 1342 *Physiology*, **136**, 3999-4009.
 1343 Valentine T.A., Hallett P.D., Binnie K., Young M.W., Squire G.R., Hawes C. & Bengough A.G.
 1344 (2012b) Soil strength and macropore volume limit root elongation rates in many UK
 1345 agricultural soils. *Annals of Botany*, **110**, 259-270.
 1346 Valentine T.A., Randall E., Wypijewski K., Chapman S., Jones J. & Oparka K.J. (2007) Delivery
 1347 of macromolecules to plant parasitic nematodes using a tobacco rattle virus vector.
 1348 *Plant Biotechnology Journal*, **5**, 827-834.
 1349 van der Weele C.M., Jiang H.S., Palaniappan K.K., Ivanov V.B., Palaniappan K. & Baskin T.I.
 1350 (2003) A new algorithm for computational image analysis of deformable motion at
 1351 high spatial and temporal resolution applied to root growth. Roughly uniform
 1352 elongation in the meristem and also, after an abrupt acceleration, in the elongation
 1353 zone. *Plant Physiology*, **132**, 1138-1148.
 1354 Veen B.W., Vannoordwijk M., Dewilligen P., Boone F.R. & Kooistra M.J. (1992) Root-soil
 1355 contact of maize, as measured by a thin-section technique .3. effects on shoot
 1356 growth, nitrate and water-uptake efficiency. *Plant and Soil*, **139**, 131-138.
 1357 Villordon A., LaBonte D. & Solis J. (2011) Using a Scanner-based Minirhizotron System to
 1358 Characterize Sweetpotato Adventitious Root Development during the Initial Storage
 1359 Root Bulking Stage. *Hortscience*, **46**, 513-517.
 1360 Vollsnes A.V., Futsaether C.M. & Bengough A.G. (2010) Quantifying rhizosphere particle
 1361 movement around mutant maize roots using time-lapse imaging and particle image
 1362 velocimetry. *European Journal of Soil Science*, **61**, 926-939.
 1363 Walter A. & Schurr U. (2005) Dynamics of leaf and root growth: Endogenous control versus
 1364 environmental impact. *Annals of Botany*, **95**, 891-900.
 1365 Walter A., Studer B. & Koelliker R. (2012) Advanced phenotyping offers opportunities for
 1366 improved breeding of forage and turf species. *Annals of Botany*, **110**, 1271-1279.
 1367 Wang Y. & Frei M. (2011) Stressed food - The impact of abiotic environmental stresses on
 1368 crop quality. *Agriculture Ecosystems & Environment*, **141**, 271-286.
 1369 Watt M., Hugenholtz P., White R. & Vinall K. (2006) Numbers and locations of native bacteria
 1370 on field-grown wheat roots quantified by fluorescence in situ hybridization (FISH).
 1371 *Environmental Microbiology*, **8**, 871-884.
 1372 Watt M., McCully M.E. & Canny M.I. (1993) Interactions in the rhizosheath. *Plant Physiology*,
 1373 **102**, 19-19.
 1374 Watt M., Moosavi S., Cunningham S.C., Kirkegaard J.A., Rebetzke G.J. & Richards R.A. (2013)
 1375 A rapid, controlled-environment seedling root screen for wheat correlates well with
 1376 rooting depths at vegetative, but not reproductive, stages at two field sites. *Annals*
 1377 *of botany*, **112**, 447-455.

- 1378 Weaver J.E. (1919) The ecological relations of roots. In: *Papers of John E. Weaver (1884-*
1379 *1956). Paper 13.*
- 1380 Wells D.M., French A.P., Naeem A., Ishaq O., Traini R., Hijazi H., . . . ,Pridmore T.P. (2012)
1381 Recovering the dynamics of root growth and development using novel image
1382 acquisition and analysis methods. *Philosophical Transactions of the Royal Society B-*
1383 *Biological Sciences*, **367**, 1517-1524.
- 1384 White P.J., George T.S., Dupuy L.X., Karley A.J., Valentine T.A., Wiesel L. & Wishart J. (2013a)
1385 Root traits for infertile soils. *Frontiers in Plant Science*, **4**, 193.
- 1386 White P.J., George T.S., Gregory P.J., Bengough A.G., Hallett P.D. & McKenzie B.M. (2013b)
1387 Matching roots to their environment. *Annals of Botany*, **112**, 207-222.
- 1388 White R.G. & Kirkegaard J.A. (2010) The distribution and abundance of wheat roots in a
1389 dense, structured subsoil - implications for water uptake. *Plant Cell and Environment*,
1390 **33**, 133-148.
- 1391 Willatt S.T. & Struss R.G. (1979a) Germination and early growth of plants studied using
1392 neutron radiography. *Annals of Botany*, **43**, 415-422.
- 1393 Willatt S.T. & Struss R.G. (1979b) Neutron radiography, a technique for studying young roots
1394 growing in soil. *Isotopes and radiation in research on soil-plant relationships*
1395 *(International Atomic Energy Agency, Vienna)*. 513-525.
- 1396 Willatt S.T., Struss R.G. & Taylor H.M. (1978) *In situ* root studies using neutron radiography.
1397 *Agronomy Journal*, **70**, 581-586.
- 1398 Wojciechowski T., Gooding M.J., Ramsay L. & Gregory P.J. (2009) The effects of dwarfing
1399 genes on seedling root growth of wheat. *Journal of Experimental Botany*, **60**, 2565-
1400 2573.
- 1401 Wu C., Wei X., Sun H.L. & Wang Z.Q. (2005) Phosphate availability alters lateral root anatomy
1402 and root architecture of *Fraxinus mandshurica* Rupr. seedlings. *Journal of Integrative*
1403 *Plant Biology*, **47**, 292-301.
- 1404 Wuyts N., Bengough A.G., Roberts T.J., Du C.J., Bransby M.F., McKenna S.J. & Valentine T.A.
1405 (2011) Automated motion estimation of root responses to sucrose in two
1406 *Arabidopsis thaliana* genotypes using confocal microscopy. *Planta*, **234**, 769-784.
- 1407 Yang Z., Downie H., Rozbicki E., Dupuy L.X. & MacDonald M.P. (2013) Light Sheet
1408 Tomography (LST) for in situ imaging of plant roots. *Optics Express*, **21**, 16239-16247.
- 1409 Zappala S., Mairhofer S., Tracy S., Sturrock C.J., Bennett M., Pridmore T. & Mooney S.J. (2013)
1410 Quantifying the effect of soil moisture content on segmenting root system
1411 architecture in X-ray computed tomography images. *Plant and Soil*, **370**, 35-45.
- 1412 Zhang H., Fritts J.E. & Goldman S.A. (2008) Image segmentation evaluation: A survey of
1413 unsupervised methods. *Computer Vision and Image Understanding*, **110**, 260-280.
- 1414 Zhu J., Ingram P.A., Benfey P.N. & Elich T. (2011) From lab to field, new approaches to
1415 phenotyping root system architecture. *Current Opinion in Plant Biology*, **14**, 310-317.
- 1416

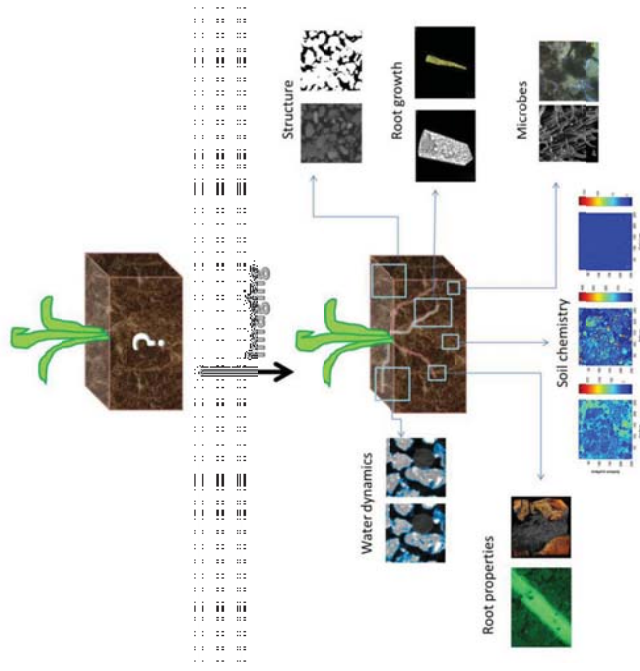


Figure 1. Visualisation of rhizosphere abiotic and biotic interactions. Interactions at the rhizosphere involve many different physical, chemical and biotic processes. This requires a range of imaging and image analysis solutions. Soil chemistry images courtesy of Simona Hapca. Microbes, (left) Downie et al. (2012), (right) with kind permission of Elsevier Limited, reproduced from Harris et al. (2002).

160x160mm (300 x 300 DPI)

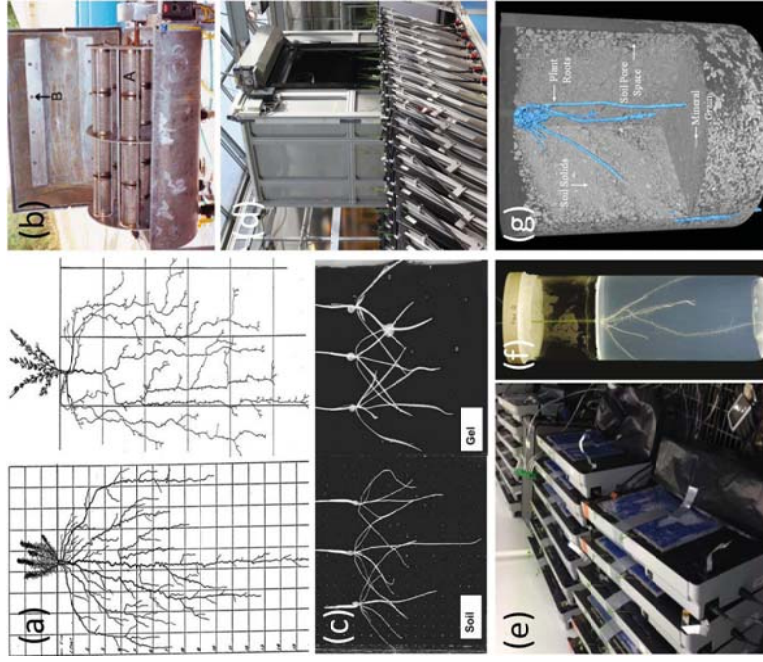


Figure 2. Root imaging from destructive harvests to 2D automated imaging systems and 3D phenotyping. Root imaging from destructive harvests to 2D automated imaging systems and 3D phenotyping of roots in soil. Imaging systems have progressed from manual tracing of roots extracted from soil through to in situ analysis of roots growing in soil. Root were initially manually extracted from soil and an image produced by tracing the roots (a). Some automated systems for extracting root from soil have been developed (b). Scanners can be used to assist in analysis and quantification of extracted roots or for capturing of root data in situ in both gel and soil systems (c, d, e). These scanner systems are conducive to automated image capture of root growth of multiple plants due to either multiple scanning points (e) or by automated movement of plant growth boxes (d). 3D analysis of roots growing in gels systems for optical imaging or in soil using for example, x-ray- μ CT imaging is also possible (f, g) (a) Manually traced root systems (Weaver, 1919). (b) Automated extraction of roots from soil (Benjamin & Nielsen, 2004). (c) Barley seedlings grown in 2D soil and gel system imaged by scanner illustrating root growth patterns (Benough et al., 2004). (d) Automated robotic phenotyping system, GROWSCREEN-Rhizo (Nagel et al., 2012). (e) Multiple automated scanner bank for automated time-lapse imaging of roots

growing on filter paper (Adu et al., 2014). (f) Roots growing in a gel based system used for 3D tomography optical imaging (Clark et al., 2011). (g) Roots in situ in soil imaged using x-ray- μ CT (Zappala et al., 2013). (a) Reproduced under open licence from DigitalCommons@University of Nebraska. (b, c, g) Reproduced with kind permission from Springer Science and Business media. (d) Reproduced with kind permission from CSIRO Publishing. (f) Reproduced with kind permission from the American Society of Plant Biologists.

160x190mm (300 x 300 DPI)

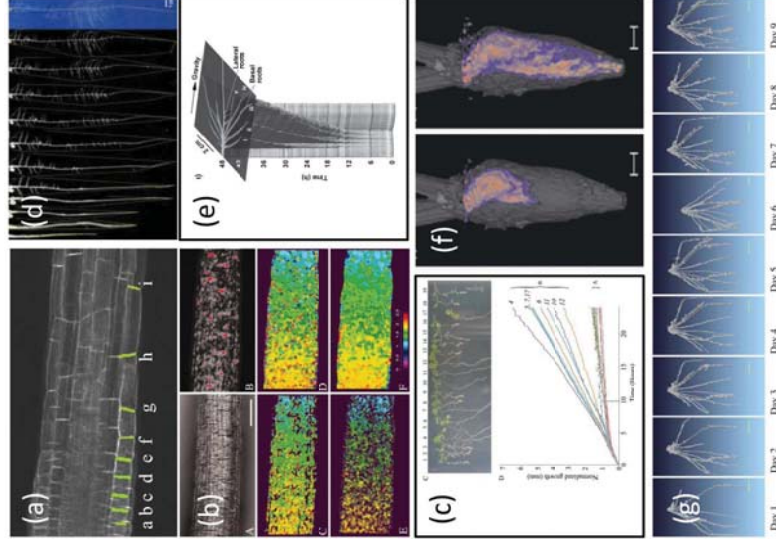


Figure 3. Analysis of Root system architecture dynamics
Analysis of root growth dynamics from cellular through to architectural scale using motion analysis (a, b) or time-lapse snap shots (c-g). (a) Motion analysis of individual cell boundaries to analyse cell expansion utilising PlantVis-R (Arabidopsis expressing GFP::LTI in the plasma membrane imaged using CLSM) (Wuyts et al., 2011). (b) Kinetic analysis of root elongation at the meristem scale using IR imaging (Van der Weele et al., 2003). (c) Automated camera based high-throughput imaging and image analysis of root elongation and curvature (French et al., 2009). (d) Automated scanner bank (see Figure 2e) based architectural analysis (previously unpublished image, (Adu et al., 2014)). (e) 3D visualisation of root architecture changes over time (Basu & Pal, 2012). (f) Analysis of C sequestration using a combination of MRI and PET imaging (Jahnke et al., 2009). (g) Repeated imaging of Rice roots in situ in soil using X-ray μ -CT imaging (Zappala et al., 2013) allowing analysis of 3D architectural dynamics in soil.
(a, g) Reproduced with kind permission from Springer Science and Business media. (b, c) Reproduced with kind permission from the American Society of Plant Biologists. (d) Previously unpublished image (e, f)

Reproduced with kind permission from John Wiley & Sons.

160x231mm (300 x 300 DPI)

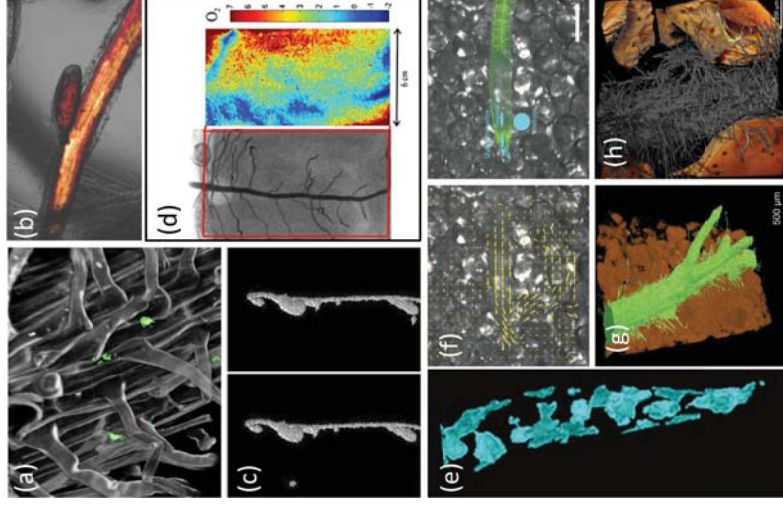


Figure 4. Imaging and image analysis of biotic and abiotic interactions at the root:rhizosphere interface. Imaging and image analysis of biotic and abiotic interactions at the root:rhizosphere interface. Visualisation of biotic interactions (a-c), chemical (d) and physical interactions (e-h). (a) GFP expressing bacterial colonies forming on roots of plants grown in transparent soil (Downie et al., 2012). (b) Heterodera schachtii feeding on roots infected with Tobacco rattle virus expressing mRFP protein to visualise the uptake of mRFP by the nematode during feeding (unpublished image - Valentine et al. (2007)). X-ray CT utilised to image Setona seeking out root nodules in an intact root:soil sample (Johnson et al., 2004). (d) Physical interactions: Neutron radiography image of roots (left) with image of oxygen gradients (right) obtained using oxygen sensitive foil (Rudolph et al., 2012). (e) Analysis of root soil contact, blue represents areas of root surface in contact with soil particles (Schmidt et al., 2012). (f) Dynamic root growth analysis using PIV showing movement of surrounding constraining growth medium in response to root penetration (Bengough et al., 2010). (g) Synchrotron data enabling visualisation of root hair contact in intact soil samples (Keyes et al., 2013). (h) Fluorescence based (CLSM) imaging to visualise root hair particle interactions in

transparent soil (Previously unpublished image - (Downie et al., 2012). (a), Reproduced under Creative Commons Attribution License. (b) Previously unpublished image. (c, e, f, g) Reproduced with kind permission from John Wiley & Sons. (d) Reproduced with kind permission from Springer Science and Business media.

160x251mm (300 x 300 DPI)

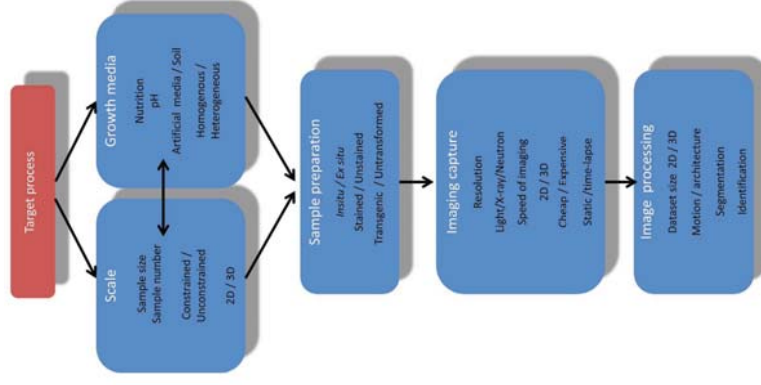


Figure 5. Decision process for root phenotyping pipeline
Phenotyping the rhizosphere via image analysis requires several inter connecting steps, each with many parameters that need to be considered. Each parameter may impact on the downstream processing of the images or may alter the number of images and the type of images that it is necessary to acquire earlier in the analysis pipeline

160x316mm (300 x 300 DPI)